



CERN-EP-2022-056
17 March 2022

**Measurements of the groomed jet radius and momentum splitting fraction
with the soft drop and dynamical grooming algorithms in pp collisions at
 $\sqrt{s} = 5.02$ TeV**

ALICE Collaboration*

Abstract

This article presents measurements of the groomed jet radius and momentum splitting fraction in pp collisions at $\sqrt{s} = 5.02$ TeV with the ALICE detector at the Large Hadron Collider. Inclusive charged-particle jets are reconstructed at midrapidity using the anti- k_T algorithm for transverse momentum $60 < p_T^{\text{ch jet}} < 80$ GeV/c. We report results using two different grooming algorithms: soft drop and, for the first time, dynamical grooming. For each grooming algorithm, a variety of grooming settings are used in order to explore the impact of collinear radiation on these jet substructure observables. These results are compared to perturbative calculations that include resummation of large logarithms at all orders in the strong coupling constant. We find good agreement of the theoretical predictions with the data for all grooming settings considered.

arXiv:2204.10246v2 [nucl-ex] 21 Jun 2023

1 Introduction

Measurements of high-energy jets produced in proton–proton collisions provide opportunities to test perturbative calculations and study non-perturbative (NP) effects in quantum chromodynamics (QCD) [1–3]. Jets also can be used to probe the properties of the quark–gluon plasma by comparing jet observables in high-energy heavy-ion collisions to reference measurements in proton–proton collisions [4–12].

Jet grooming techniques, such as soft drop [13–15] and dynamical grooming [16–19], reduce the magnitude of non-perturbative contributions to jet substructure cross sections in pp collisions by selectively removing soft large-angle radiation. This allows for well-controlled comparisons of measurements to perturbative QCD (pQCD) calculations. Grooming techniques have also previously been applied to heavy-ion collisions, in order to explore whether the quark–gluon plasma modifies the hard substructure of jets [19–29]. Several measurements of groomed jet observables have been made in pp and heavy-ion collisions at the LHC and RHIC [30–37], as well as in e^+e^- collisions [38]. The benefits of different jet grooming algorithms remain a topic of ongoing study, since different grooming algorithms have different perturbative structure and offer different flexibility via grooming parameters that can be adapted to specific physics goals in either proton–proton or heavy-ion collisions (see e.g. Refs. [19, 26, 29]). In this article, we explore both the soft drop and dynamical grooming algorithms, and test the ability of pQCD calculations to describe their behavior for a variety of grooming parameters.

Jet grooming algorithms rely on procedures to recluster the constituents of reconstructed jets into a structure that better isolates perturbative emissions in the jet. One such structure is the primary Lund plane, which approximately represents the angular and momentum phase space of partonic emissions off the leading hard-scattered parton. The soft drop and dynamical grooming algorithms each identify a single splitting in the primary Lund plane [39] that satisfies a grooming condition. The two algorithms are further described in Section 3. In this article, we consider two observables that define the kinematics of the identified splitting: z_g , the groomed jet momentum splitting fraction, and θ_g , the (scaled) groomed jet radius, as shown in Fig. 1. The groomed jet momentum splitting fraction is defined as the fraction of transverse momentum (p_T) relative to the beam that the sub-leading prong in the splitting carries relative to its parent:

$$z_g \equiv \frac{p_{T,\text{subleading}}}{p_{T,\text{leading}} + p_{T,\text{subleading}}}. \quad (1)$$

The (scaled) groomed jet radius is defined as the angular distance between the two prongs of the identified hard splitting

$$\theta_g \equiv \frac{R_g}{R} \equiv \frac{\sqrt{\Delta y^2 + \Delta\phi^2}}{R}, \quad (2)$$

where R is the jet radius and R_g is the rapidity–azimuth (y – ϕ) separation of the identified splitting.

The soft drop z_g and θ_g distributions have recently been calculated in pp collisions at Next-to-Leading Logarithmic (NLL') accuracy [40, 41]. Measurements of z_g and θ_g serve to test these analytical predictions, in particular, the role of beyond-LL pQCD effects, as well as constrain the role of non-perturbative effects. Moreover, by measuring these observables for a variety of grooming conditions β (see Section 3.1 for further details), one can systematically study the role of collinear radiation in jet substructure, since increasing β removes less and less collinear radiation in the grooming process. Measurements of both z_g and θ_g for $\beta = 0, 1$, and 2 have been performed by the ATLAS Collaboration [32] for dijet events with leading $p_T^{\text{jet}} > 300$ GeV/ c , and several measurements of z_g and θ_g have been performed for $\beta = 0$ across a wide range of jet p_T [31, 33, 36, 38]. In this article, we complement these studies by measuring z_g and θ_g for $\beta = 0, 1$, and 2 for $60 < p_T^{\text{ch jet}} < 80$ GeV/ c .

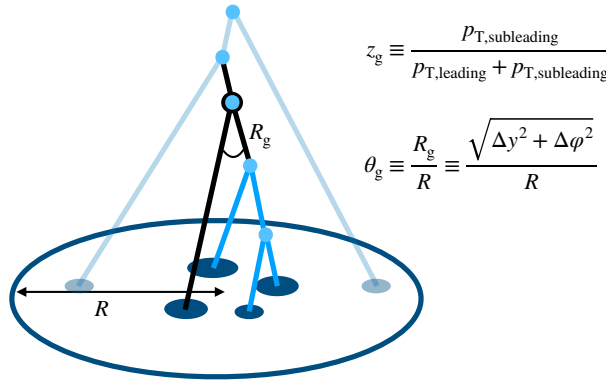


Figure 1: Graphical representation of the angularly-ordered Cambridge–Aachen reclustering of jet constituents and subsequent grooming procedure, with the identified splitting denoted in black and the splittings that were groomed away in light blue.

The dynamically groomed z_g and θ_g distributions have recently been calculated in pp collisions at Next-to-Next-to-Double Logarithm (N²DL) accuracy [16, 18]. In this article, we perform the first measurement of dynamically groomed jet substructure observables, providing the first test of these calculations.

We report measurements in pp collisions at center-of-mass collision energy $\sqrt{s} = 5.02$ TeV with the ALICE detector. Charged-particle jets are reconstructed in the pseudorapidity range $|\eta_{\text{jet}}| < 0.5$ for jet radius $R = 0.4$ with $60 < p_{\text{T}}^{\text{ch,jet}} < 80$ GeV/ c . The z_g and θ_g distributions are measured using both the soft drop and dynamical grooming procedures, each with a variety of grooming settings. These results are compared to pQCD calculations as well as the PYTHIA8 [42, 43] Monte Carlo (MC) event generator. While track-based jet observables are collinear-unsafe [44–46], they can be measured with greater precision than calorimeter-based jet observables, and recent measurements have demonstrated that for many substructure observables track-based distributions are compatible with the corresponding collinear-safe distributions [32]. Comparisons of theoretical calculations to our track-based jet substructure measurements are discussed further in Section 5.

2 Experimental setup and data sets

A description of the ALICE detector and its performance can be found in Refs. [47, 48]. The pp data set used in this analysis was collected in 2017 during LHC Run 2 at $\sqrt{s} = 5.02$ TeV using a minimum-bias trigger defined by the coincidence of the signals from two scintillator arrays in the forward region (V0 detectors) [49]. The event selection includes a primary vertex selection, where the primary vertex is required to be within 10 cm from the center of the detector along the beam direction. Events with more than one reconstructed primary vertex were classified as pileup and rejected [50]. After these selections, the pp data sample contains 870 million events and corresponds to an integrated luminosity of 18.0 ± 0.4 nb⁻¹ [51].

The analysis uses charged-particle tracks reconstructed with information from the Time Projection Chamber (TPC) [52] and the Inner Tracking System (ITS) [53]. Two types of tracks are defined: global tracks and complementary tracks. Global tracks are required to include at least one hit in the silicon pixel detector (SPD) comprising the first two layers of the ITS and to satisfy several track quality selections. Complementary tracks are all those satisfying all the selection criteria of global tracks except for the request of a point in the SPD. They are refitted using the primary vertex to constrain their trajectory in order to preserve a good momentum resolution, especially at high transverse momentum. Including this second class of tracks ensures approximately uniform azimuthal acceptance, while preserving similar p_{T} resolution to tracks with SPD hits. Tracks with $0.15 < p_{\text{T}} < 100$ GeV/ c are accepted over pseudorapidity range $|\eta| < 0.9$ and azimuthal angle $0 < \varphi < 2\pi$.

The instrumental performance of the detector is estimated with a MC simulation done using PYTHIA8 [42] with the Monash 2013 tune [43] for the event generation and GEANT3 [54] for the transport code propagating particles through the simulated ALICE apparatus. The tracking efficiency in pp collisions is approximately 67% at track $p_T = 0.15$ GeV/ c , and rises to approximately 84% at $p_T = 1$ GeV/ c , and remains above 75% at higher p_T . The momentum resolution $\sigma(p_T)/p_T$ was estimated from the covariance matrix of the track fit [48], and is approximately 1% at track $p_T = 1$ GeV/ c and 4% at $p_T = 50$ GeV/ c .

3 Analysis method

Jets are reconstructed from charged-particle tracks with FastJet 3.2.1 [55] using the anti- k_T algorithm with E -scheme recombination with resolution parameter $R = 0.4$ [56, 57]. All tracks are assigned a mass equal to the π^\pm meson mass. The jet axis is required to be within the fiducial volume of the TPC, $|\eta_{\text{jet}}| < 0.5$, where η_{jet} is the jet pseudorapidity. The jet reconstruction performance for this data set is described in Ref. [30]. The underlying event (UE) consists of approximately $p_T = 1$ GeV/ c per jet, and is not subtracted. Therefore, UE corrections must be included in theoretical calculations when comparing to the data.

3.1 Grooming algorithms

The soft drop and dynamical grooming algorithms identify a single splitting in the primary Lund plane [39] that satisfies a grooming condition. The i^{th} splitting in the primary Lund plane is defined by

$$\begin{aligned} z_i &\equiv \frac{p_{T,\text{subleading},i}}{p_{T,\text{leading},i} + p_{T,\text{subleading},i}}, \\ \theta_i &\equiv \frac{\Delta R_i}{R}, \end{aligned} \quad (3)$$

where $\Delta R_i = \sqrt{\Delta y_i^2 + \Delta \phi_i^2}$ is the rapidity-azimuth separation of the i^{th} splitting. Note that when reconstructing the primary Lund plane, one must choose a reclustering radius $R_{\text{recluster}}$; for soft drop $R_{\text{recluster}} = R$ is used, which results in $\theta_g \leq 1$, whereas for our implementation of dynamical grooming $R_{\text{recluster}} = \infty$ is used, which results in $\theta_g > 1$ for <1% of cases (which we neglect).

In the soft drop grooming algorithm, the grooming condition is given by

$$z_i > z_{\text{cut}} \theta_i^\beta, \quad (4)$$

where z_{cut} and the exponent β are tunable free parameters of the grooming algorithm. The first such splitting to pass the grooming condition defines the soft drop groomed jet splitting. As the grooming parameter β increases, the quantity $z_{\text{cut}} \theta_i^\beta$ becomes small for collinear radiation. This causes the algorithm to be less likely to drop collinear radiation — corresponding to less grooming overall, and particularly less grooming for collinear radiation. Note that for the values $\beta \geq 0$ considered here, z_g is Sudakov safe [15] and θ_g is infrared-collinear safe [40].

The dynamical grooming algorithm, on the other hand, identifies the splitting that maximizes

$$z_i(1 - z_i)p_{T,i}\theta_i^a \quad (5)$$

over all splittings in the primary Lund plane, where the exponent a is a continuous free parameter. The grooming parameter a defines the density with which the phase space of the Lund plane is groomed away. The case $a \rightarrow 0$ selects the splitting with largest z , and is somewhat similar to soft drop with $\beta = 0$, which grooms away splittings below a certain z . The case $a = 1$ selects the splitting with largest transverse momentum, and is roughly analogous to soft drop with $\beta = -1$, which grooms away splittings

below a certain transverse momentum (see Ref. [16] for further details). Since the grooming condition in dynamical grooming defines a maximum rather than an explicit cut (as in the case of soft drop), every dynamically groomed jet will always return a splitting, whereas in soft drop it is possible that a jet does not contain any splitting satisfying the grooming condition.

3.2 Corrections

The reconstructed $p_T^{\text{ch jet}}$ and $z_g(\theta_g)$ differ from their true values due to tracking inefficiency, particle–material interactions, and track p_T resolution. To account for these effects, events are simulated using PYTHIA8 Monash 2013 [42, 43] for the event generation and GEANT3 [54] for the transport code propagating particles through the simulated ALICE apparatus, as described in Section 2. The truth-level jets are constructed from the charged primary particles of the PYTHIA8 event, defined as all particles with a mean proper lifetime larger than 1 cm/c, and excluding the decay products of these particles [58]. A 4D response matrix is constructed that describes the detector response in $p_T^{\text{ch jet}}$ and z_g (and similarly for θ_g): $R(p_{T,\text{det}}^{\text{ch jet}}, p_{T,\text{truth}}^{\text{ch jet}}, z_{g,\text{det}}, z_{g,\text{truth}})$, where $p_{T,\text{det}}^{\text{ch jet}}$ is the detector-level $p_T^{\text{ch jet}}$ and $p_{T,\text{truth}}^{\text{ch jet}}$ is the truth-level $p_T^{\text{ch jet}}$.

Then, a 2D unfolding is performed in $p_T^{\text{ch jet}}$ and z_g using the iterative Bayesian unfolding algorithm [59, 60] implemented in the RooUnfold package [61]. The distributions are corrected for “misses”, in which a jet exists inside the considered truth level range but not inside the detector level range. The rate of “fakes”, in which a jet exists inside the considered detector level range but not inside the truth level range, is negligible. The number of iterations, which sets the strength of regularization, is chosen by minimizing the quadrature sum of the statistical and systematic unfolding uncertainties. This results in the optimal number of iterations equal to 3 in all cases.

To validate the performance of the unfolding procedure, refolding tests are performed, in which the response matrix is multiplied by the unfolded solution and compared to the original detector-level spectrum. Closure tests are also performed, in which the shape of the generated MC spectrum is modified to account for the fact that the true distribution may be different from the MC spectrum. In all cases, successful closure within statistical and systematic uncertainties is achieved.

4 Systematic uncertainties

Systematic uncertainties due to the tracking efficiency, the unfolding procedure, and the MC generator model dependence are considered. Table 1 summarizes the systematic uncertainty contributions from each of these sources. The total systematic uncertainty is calculated as the sum in quadrature of all of the individual systematic uncertainties described below.

The systematic uncertainty due to the uncertainty in the tracking efficiency is evaluated using random rejection of additional tracks in the jet finding. The tracking efficiency uncertainty, estimated from the variation of the track selection criteria and a detailed study of the ITS–TPC track-matching efficiency uncertainty, is 4%. In order to assign a systematic uncertainty to the nominal result, an alternative response matrix is constructed by randomly rejecting an additional 4% of tracks in jet finding, and the unfolding procedure is repeated. This result is compared to the nominal result, with the differences in each bin taken as the systematic uncertainty. The uncertainty on the track momentum resolution is a sub-leading effect to the tracking efficiency and is taken to be negligible.

Four sets of variations of the unfolding procedure are performed in order to estimate the systematic uncertainty arising from the unfolding regularization procedure.

- The number of iterations in the unfolding procedure is varied by ± 2 units, chosen based on studies of the rate of convergence of the unfolding procedure. The average difference with respect to the

Table 1: Summary of systematic uncertainties on unfolded z_g and θ_g distributions for $60 < p_T^{\text{ch jet}} < 80$ GeV/ c . The ranges correspond to the minimum and maximum systematic uncertainties obtained.

| | | Relative uncertainty (%) | | | |
|-----------------------------------|-------------|--------------------------|-----------|-----------|-------|
| Soft drop, $z_{\text{cut}} = 0.1$ | | Tracking efficiency | Unfolding | Generator | Total |
| z_g | $\beta = 0$ | 0–2% | 0–4% | 0–1% | 2–5% |
| | $\beta = 1$ | 0–4% | 0–4% | 0–3% | 1–6% |
| | $\beta = 2$ | 0–3% | 1–5% | 0–5% | 2–7% |
| θ_g | $\beta = 0$ | 2–8% | 2–6% | 0–4% | 3–9% |
| | $\beta = 1$ | 2–10% | 0–5% | 0–3% | 2–12% |
| | $\beta = 2$ | 2–11% | 1–6% | 0–5% | 2–13% |
| Dynamical grooming | | Tracking efficiency | Unfolding | Generator | Total |
| z_g | $a = 0.1$ | 0–14% | 2–10% | 0–4% | 2–17% |
| | $a = 1.0$ | 0–5% | 1–4% | 0–2% | 1–5% |
| | $a = 2.0$ | 0–4% | 1–5% | 0–3% | 2–7% |
| θ_g | $a = 0.1$ | 0–6% | 1–5% | 0–4% | 2–8% |
| | $a = 1.0$ | 1–9% | 1–5% | 0–3% | 2–10% |
| | $a = 2.0$ | 0–8% | 1–3% | 0–7% | 2–11% |

nominal result is taken as the systematic uncertainty.

- The prior distribution is scaled by a power law in $p_T^{\text{ch jet}}$ and by $p_T^{\pm 0.5} z_g^{\pm 0.5}$ for the z_g analysis. For the θ_g analysis, a linear scaling in θ_g by $\pm 50\%$ over its reported range, scaling by $p_T^{\pm 0.5} [1 \pm 0.5(2\theta_g - 1)]$, is applied. The average difference between the result unfolded with this prior and the original is taken as the systematic uncertainty.
- The binnings in z_g and θ_g are varied to be finer and coarser than the nominal binning.
- The lower bound in the detector level charged-particle jet transverse momentum $p_{T,\text{det}}^{\text{ch jet}}$ range is extended up and down by 5 GeV/ c .

The total unfolding systematic uncertainty is then the standard deviation of the variations, $\sqrt{\sum_{i=1}^N \sigma_i^2 / N}$, where $N = 4$ and σ_i is the systematic uncertainty due to a single group of variations, since they each comprise independent estimates of the same underlying systematic uncertainty in the regularization.

The systematic uncertainty due to the model dependence of the generator used to construct the response matrix is estimated by comparing results obtained with PYTHIA8 Monash 2013 [42, 43] to that obtained with Herwig7 (default tune) [62]. The tracking efficiency and track p_T resolution are parameterized using fast simulations and response matrices are built using these two generators. These response matrices are then used to unfold the measured data, and the differences between the two unfolded results in each interval are taken as a symmetric uncertainty.

5 Results

We report the z_g and θ_g distributions in the $p_T^{\text{ch jet}}$ interval between 60 and 80 GeV/ c . All presented results use $R = 0.4$ jets reconstructed from charged particles at midrapidity, and are corrected for detector effects. The distributions are reported as normalized differential cross sections,

$$\frac{1}{\sigma_{\text{jet}}} \frac{d\sigma}{dz_g} = \frac{1}{N_{\text{jet}}} \frac{dN}{dz_g}, \quad (6)$$

where N_{jet} (σ_{jet}) is the number (cross section) of inclusive charged-particle jets within the given $p_T^{\text{ch jet}}$ interval, and N (σ) is the number (cross section) of groomed splittings. The same normalization as in

Eq. 6 is used for θ_g . With this normalization, the integral of Eq. 6 is equal to the fraction of jets that pass the grooming condition.

5.1 Soft drop

Figures 2 and 3 show the measured z_g and θ_g distributions for jets with soft drop grooming for grooming parameters $z_{\text{cut}} = 0.1$ and $\beta = 0, 1$, and 2. The z_g distributions fall with increasing z_g , as is typical of the Altarelli–Parisi splitting functions [63]. The z_g distribution for $\beta = 0$ cannot populate $z_g < 0.1$ due to the grooming condition. However, for $\beta > 0$ it is possible for a sufficiently narrow splittings with $z_g < z_{\text{cut}}$ to pass the grooming condition. The z_g distributions are generally described by PYTHIA8 [42] within approximately 20%. The θ_g distributions exhibit a peak at increasingly large θ_g as β increases, due to the angular component in the grooming condition. The θ_g distributions are described by PYTHIA8 [42] typically within 20% but with deviations at low θ_g up to approximately 50%. Due to ill-defined perturbative accuracy in general-purpose MC generators such as PYTHIA and the fact that they are highly tuned to reproduce data, including jet-related observables [43], it is difficult to draw detailed physics conclusions from their comparison to data. Because of this, we instead turn our attention to comparisons with analytical calculations based on pQCD, where deeper insight can be obtained.

Theoretical calculations with soft drop grooming have been carried out within the Soft-Collinear Effective Theory (SCET) framework [64] for θ_g [40] and z_g [41]. These calculations include all-order resummations of large logarithms to NLL' accuracy [40]. In order to compare these parton-jet predictions to our measurement using charged-particle jets, a ‘‘forward folding’’ procedure is applied to account for hadronization and charged-particle effects, followed by a bin-by-bin scaling to account for Multi-Parton Interactions. These corrections are carried out following the procedure outlined in Ref. [30]. Given that the scale $\theta_g z_g p_T R$ becomes non-perturbative at low θ_g , and that our measurements of the z_g distribution do not include a lower cutoff in θ_g , we forgo these comparisons for the z_g distribution and refer the reader to Ref. [41]. Instead, we focus on comparison of the measured θ_g distribution to the SCET calculations.

Figure 4 compares the measured θ_g distributions with pQCD calculations based on SCET [40] using either PYTHIA8 [42] or Herwig7 [62] to account for non-perturbative corrections. The PYTHIA8 and Herwig7 corrections show generally similar behavior. Systematic uncertainties on the analytical predictions are estimated by systematically varying combinations of scales that emerge in the calculation. The softest of these scales determines a transition between the perturbative and non-perturbative regimes:

$$\theta_g^{\text{NP}} \lesssim \left(\frac{\Lambda}{z_{\text{cut}} p_T R} \right)^{\frac{1}{1+\beta}}, \quad (7)$$

where Λ is the energy scale at which α_s becomes non-perturbative. This transition is indicated by a dashed vertical blue line at $\Lambda = 1 \text{ GeV}/c$, taking p_T to be the weighted average $p_T^{\text{ch jet}}$ in the considered interval scaled by 20% to approximately translate the p_T scale from charged-particle jets to full jets. The cross section is normalized according to the integral of the distribution in the perturbative region,

$$\frac{1}{\sigma_{\theta_g > \theta_g^{\text{NP}}}} \frac{d\sigma}{d\theta_g}, \quad \text{where} \quad \sigma_{\theta_g > \theta_g^{\text{NP}}} = \int_{\theta_g^{\text{NP}}}^1 \frac{d\sigma}{d\theta_g} d\theta_g. \quad (8)$$

The measured θ_g distributions agree with the SCET calculations within uncertainties in the perturbative region (i.e. to the right of the dashed line), whereas divergence is seen at low values of θ_g , where non-perturbative effects dominate and the perturbative calculation is expected to break down. This holds for all values of β . Note that the perturbative regime contains an increasingly small fraction of the distribution as β grows, which demonstrates that at these $p_T^{\text{ch jet}}$ values, the majority of the θ_g distribution can only be captured by pQCD for sufficiently small β .

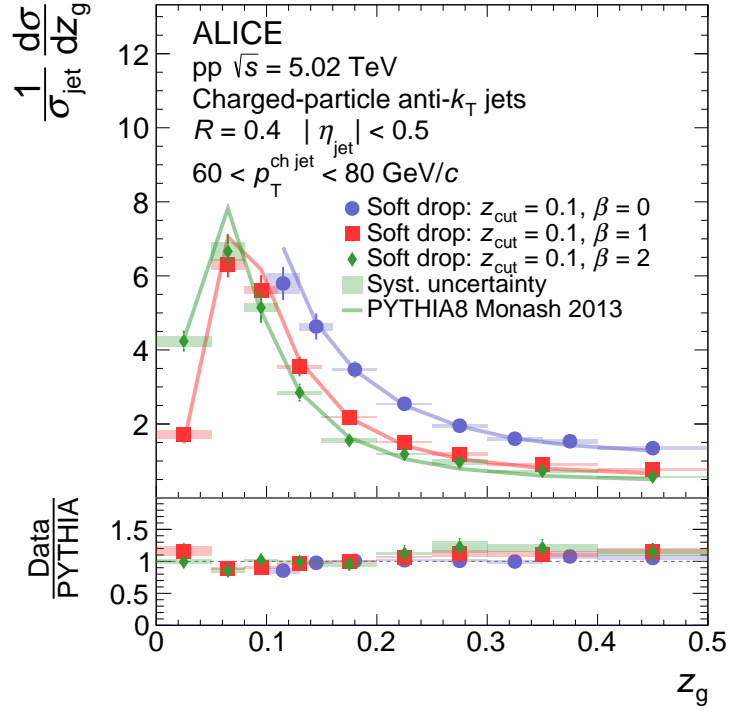


Figure 2: ALICE measurements of z_g distributions in pp collisions at $\sqrt{s} = 5.02$ TeV with soft drop for three values of the grooming parameter β , compared with PYTHIA8 Monash 2013 [42,43] calculations.

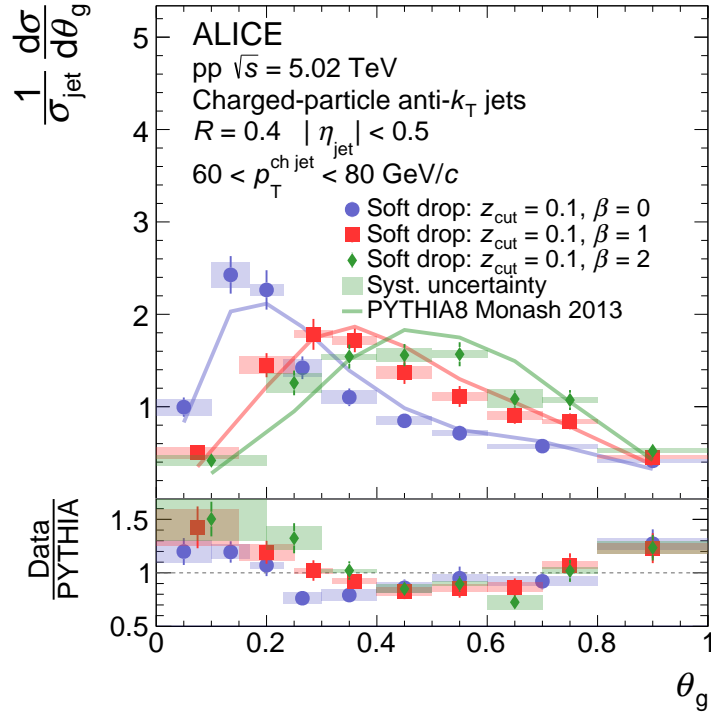


Figure 3: ALICE measurements of θ_g distributions in pp collisions at $\sqrt{s} = 5.02$ TeV with soft drop for three values of the grooming parameter β , compared with PYTHIA8 Monash 2013 [42,43] calculations.

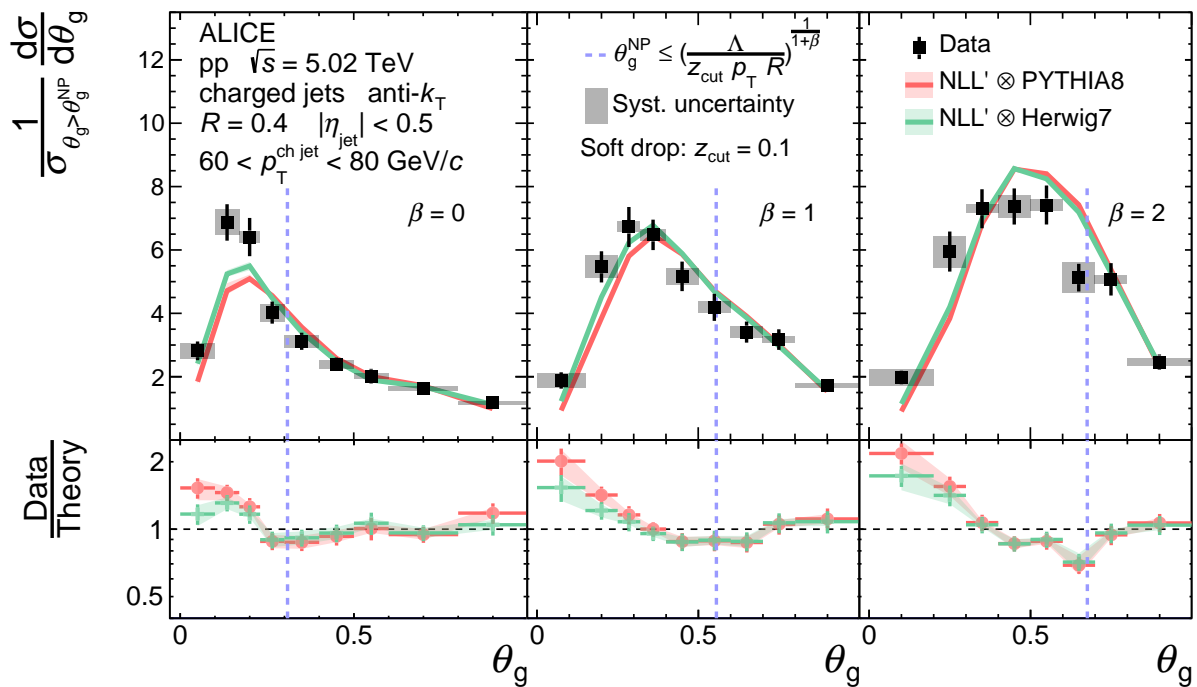


Figure 4: ALICE measurements of θ_g distributions in pp collisions at $\sqrt{s} = 5.02$ TeV with soft drop, compared with NLL' predictions carried out with SCET [40] and corrected for non-perturbative effects using either PYTHIA8 [42] or Herwig7 [62]. The distributions are normalized such that the integral of the perturbative region defined by $\theta_g > \theta_g^{\text{NP}}$ (to the right of the dashed vertical blue line) is unity. The non-perturbative scale in Eq. 7 is taken to be $\Lambda = 1$ GeV/c. In determining the normalization, intervals that overlap with the dashed blue line are considered to be in the non-perturbative (left) region.

5.2 Dynamical grooming

Figures 5 and 6 show the z_g and θ_g distributions in pp collisions for jets with dynamical grooming for several values of the grooming parameter a . For small values of a , the grooming condition favors splittings with symmetric longitudinal momenta, which is reflected in the distributions skewing towards large z_g and small θ_g . As a increases, the grooming condition favors splittings with large angular separation, which is reflected in the distributions skewing towards small z_g and large θ_g . The results are compared with PYTHIA8 Monash 2013 [42, 43], which generally describes the data within approximately 20%.

In Figs. 7 and 8, we compare the z_g and θ_g distributions, respectively, to pQCD calculations described in Ref. [18]. The theoretical calculations include non-perturbative corrections based on MC event generators, which are implemented in Ref. [18]. The theoretical uncertainty bands account for scale variations together with non-perturbative effects, the latter generally being the dominant contribution. The calculations generally describe the data within the precision of the statistical and systematic uncertainties of the data and the theoretical uncertainties of the calculation, demonstrating that pQCD predictions, when coupled with corrections for non-perturbative effects, provide a sufficient description of the data even at the moderate $p_T^{\text{ch jet}}$ considered here.

6 Conclusions

We have presented new measurements of the groomed jet radius and momentum splitting fraction in pp collisions at $\sqrt{s} = 5.02$ TeV with the ALICE detector at the Large Hadron Collider. We studied two grooming algorithms, soft drop and dynamical grooming, each with a variety of grooming settings in order to study their impact on soft- and wide-angle radiation. These studies have provided the first mea-

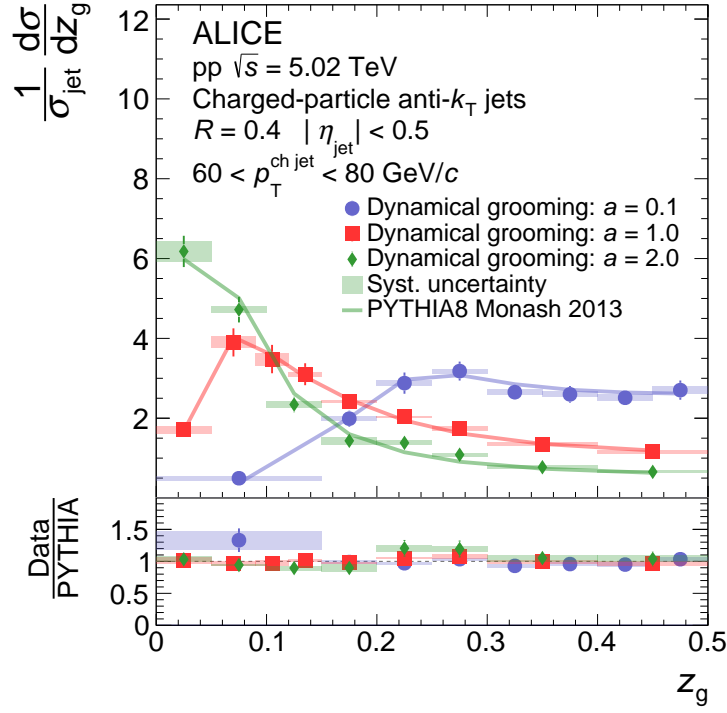


Figure 5: ALICE measurements of z_g distributions in pp collisions at $\sqrt{s} = 5.02$ TeV with dynamical grooming [16] for three values of the grooming parameter a , compared with PYTHIA8 Monash 2013 [42, 43] calculations.

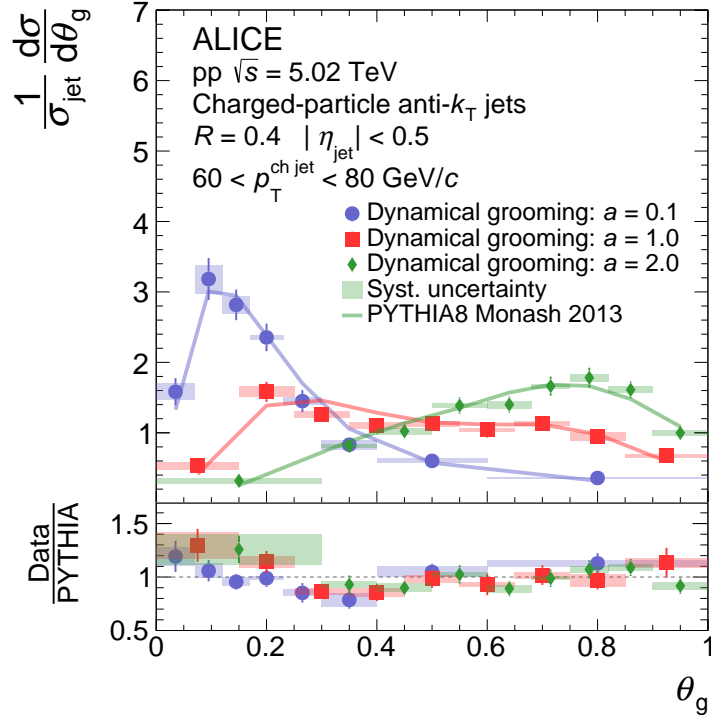


Figure 6: ALICE measurements of θ_g distributions in pp collisions at $\sqrt{s} = 5.02$ TeV with dynamical grooming [16] for three values of the grooming parameter a , compared with PYTHIA8 Monash 2013 [42, 43] calculations.

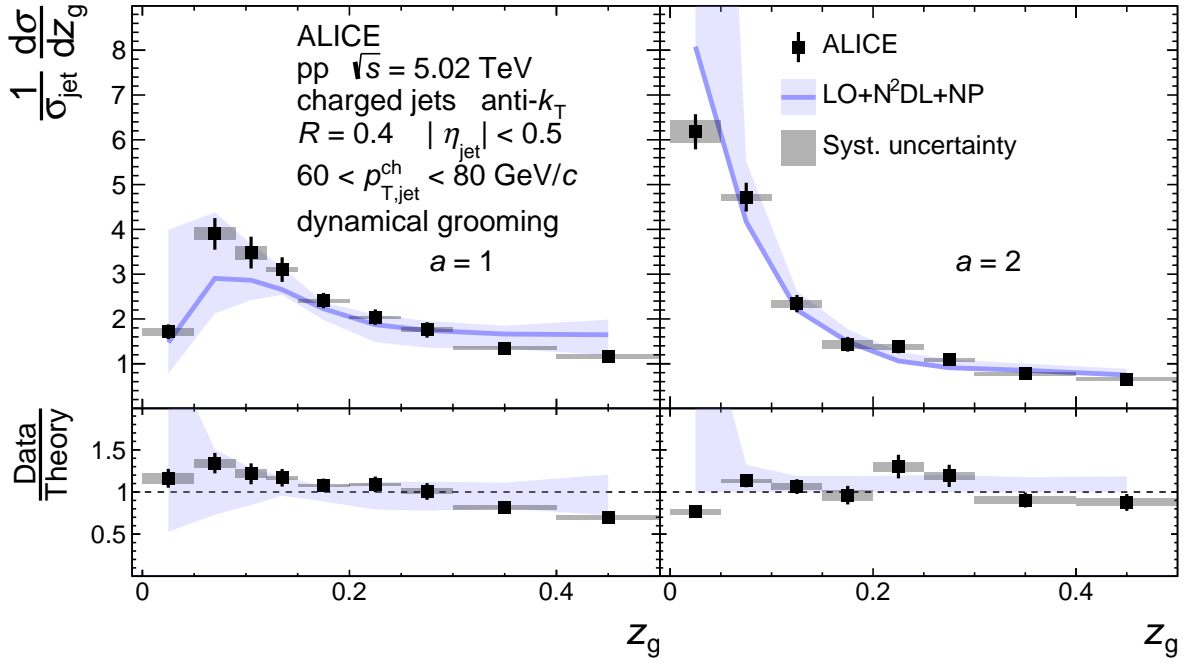


Figure 7: ALICE measurements of z_g distributions in pp collisions at $\sqrt{s} = 5.02$ TeV with dynamical grooming for two values of the grooming parameter a , compared with pQCD calculations [16, 18].

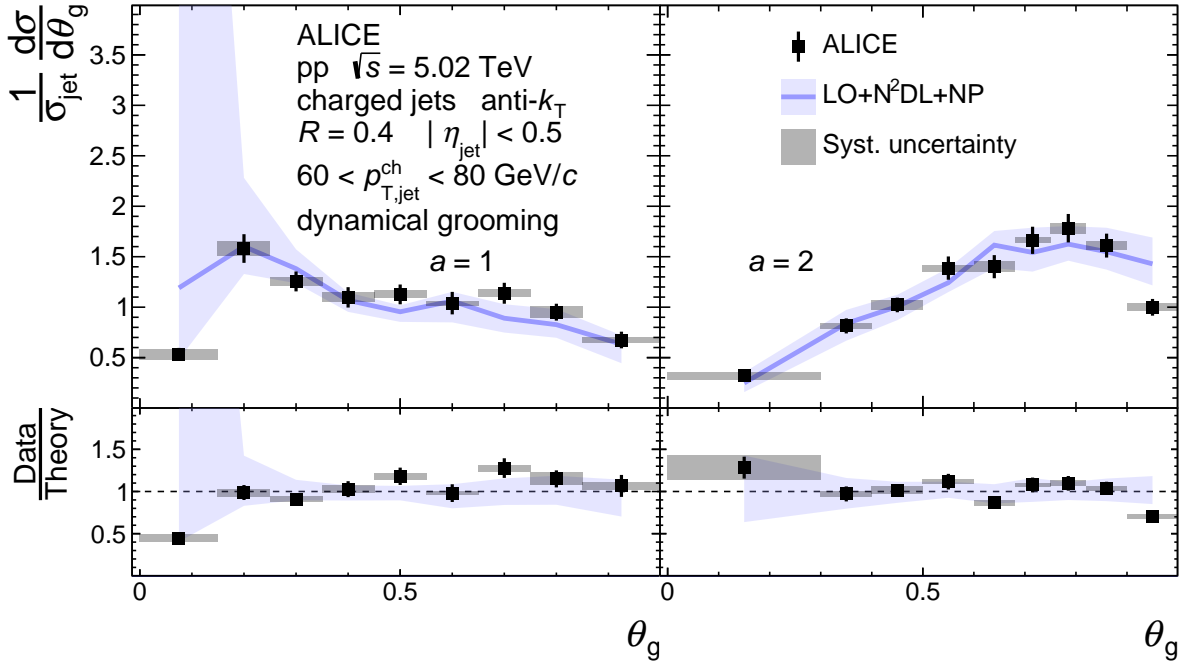


Figure 8: ALICE measurements of θ_g distributions in pp collisions at $\sqrt{s} = 5.02$ TeV with dynamical grooming for two values of the grooming parameter a , compared with pQCD calculations [16, 18].

surement of a jet substructure observable with the dynamical grooming procedure. We compared these results to perturbative calculations that include resummation of large logarithms at all orders in the strong coupling constant, and generally found agreement of the theoretical predictions with the data in the perturbative regime. This conclusion holds for all grooming settings considered. However, the soft drop θ_g distributions increasingly deviate from the perturbative calculations at small θ_g as the grooming pa-

parameter β is increased (corresponding to grooming away less collinear radiation). This is in accordance with the predicted limitation of the perturbative calculation in describing the non-perturbative region, and provides guidance for the regimes within which perturbative QCD can be used to describe the observables. These measurements can be used both to test future perturbative calculations and models of non-perturbative effects, and can serve as a baseline reference for future measurements in heavy-ion collisions.

Acknowledgements

We gratefully acknowledge Paul Caucal, Kyle Lee, Felix Ringer, and Alba Soto-Ontoso, and Adam Takacs for providing theoretical predictions.

The ALICE Collaboration would like to thank all its engineers and technicians for their invaluable contributions to the construction of the experiment and the CERN accelerator teams for the outstanding performance of the LHC complex. The ALICE Collaboration gratefully acknowledges the resources and support provided by all Grid centres and the Worldwide LHC Computing Grid (WLCG) collaboration. The ALICE Collaboration acknowledges the following funding agencies for their support in building and running the ALICE detector: A. I. Alikhanyan National Science Laboratory (Yerevan Physics Institute) Foundation (ANSL), State Committee of Science and World Federation of Scientists (WFS), Armenia; Austrian Academy of Sciences, Austrian Science Fund (FWF): [M 2467-N36] and Nationalstiftung für Forschung, Technologie und Entwicklung, Austria; Ministry of Communications and High Technologies, National Nuclear Research Center, Azerbaijan; Conselho Nacional de Desenvolvimento Científico e Tecnológico (CNPq), Financiadora de Estudos e Projetos (Finep), Fundação de Amparo à Pesquisa do Estado de São Paulo (FAPESP) and Universidade Federal do Rio Grande do Sul (UFRGS), Brazil; Bulgarian Ministry of Education and Science, within the National Roadmap for Research Infrastructures 2020;2027 (object CERN), Bulgaria; Ministry of Education of China (MOEC), Ministry of Science & Technology of China (MSTC) and National Natural Science Foundation of China (NSFC), China; Ministry of Science and Education and Croatian Science Foundation, Croatia; Centro de Aplicaciones Tecnológicas y Desarrollo Nuclear (CEADEN), Cubaenergía, Cuba; Ministry of Education, Youth and Sports of the Czech Republic, Czech Republic; The Danish Council for Independent Research | Natural Sciences, the VILLUM FONDEN and Danish National Research Foundation (DNRF), Denmark; Helsinki Institute of Physics (HIP), Finland; Commissariat à l’Energie Atomique (CEA) and Institut National de Physique Nucléaire et de Physique des Particules (IN2P3) and Centre National de la Recherche Scientifique (CNRS), France; Bundesministerium für Bildung und Forschung (BMBF) and GSI Helmholtzzentrum für Schwerionenforschung GmbH, Germany; General Secretariat for Research and Technology, Ministry of Education, Research and Religions, Greece; National Research, Development and Innovation Office, Hungary; Department of Atomic Energy Government of India (DAE), Department of Science and Technology, Government of India (DST), University Grants Commission, Government of India (UGC) and Council of Scientific and Industrial Research (CSIR), India; National Research and Innovation Agency - BRIN, Indonesia; Istituto Nazionale di Fisica Nucleare (INFN), Italy; Japanese Ministry of Education, Culture, Sports, Science and Technology (MEXT) and Japan Society for the Promotion of Science (JSPS) KAKENHI, Japan; Consejo Nacional de Ciencia (CONACYT) y Tecnología, through Fondo de Cooperación Internacional en Ciencia y Tecnología (FONCICYT) and Dirección General de Asuntos del Personal Académico (DGAPA), Mexico; Nederlandse Organisatie voor Wetenschappelijk Onderzoek (NWO), Netherlands; The Research Council of Norway, Norway; Commission on Science and Technology for Sustainable Development in the South (COMSATS), Pakistan; Pontificia Universidad Católica del Perú, Peru; Ministry of Education and Science, National Science Centre and WUT ID-UB, Poland; Korea Institute of Science and Technology Information and National Research Foundation of Korea (NRF), Republic of Korea; Ministry of Education and Scientific Research, Institute of Atomic Physics, Ministry of Research and Innovation and Institute of Atomic Physics and

University Politehnica of Bucharest, Romania; Ministry of Education, Science, Research and Sport of the Slovak Republic, Slovakia; National Research Foundation of South Africa, South Africa; Swedish Research Council (VR) and Knut & Alice Wallenberg Foundation (KAW), Sweden; European Organization for Nuclear Research, Switzerland; Suranaree University of Technology (SUT), National Science and Technology Development Agency (NSTDA), Thailand Science Research and Innovation (TSRI) and National Science, Research and Innovation Fund (NSRF), Thailand; Turkish Energy, Nuclear and Mineral Research Agency (TENMAK), Turkey; National Academy of Sciences of Ukraine, Ukraine; Science and Technology Facilities Council (STFC), United Kingdom; National Science Foundation of the United States of America (NSF) and United States Department of Energy, Office of Nuclear Physics (DOE NP), United States of America. In addition, individual groups or members have received support from: Marie Skłodowska Curie, Strong 2020 - Horizon 2020, European Research Council (grant nos. 824093, 896850, 950692), European Union; Academy of Finland (Center of Excellence in Quark Matter) (grant nos. 346327, 346328), Finland; Programa de Apoyos para la Superación del Personal Académico, UNAM, Mexico.

References

- [1] A. J. Larkoski, I. Moulton, and B. Nachman, “Jet Substructure at the Large Hadron Collider: A Review of Recent Advances in Theory and Machine Learning”, *Phys. Rept.* **841** (2020) 1–63, arXiv:1709.04464 [hep-ph].
- [2] R. Kogler *et al.*, “Jet Substructure at the Large Hadron Collider: Experimental Review”, *Rev. Mod. Phys.* **91** (2019) 045003, arXiv:1803.06991 [hep-ex].
- [3] S. Marzani, G. Soyez, and M. Spannowsky, “Looking inside jets: an introduction to jet substructure and boosted-object phenomenology”, *Lecture Notes in Physics* **958** (2019), arXiv:1901.10342 [hep-ph].
- [4] J. D. Bjorken, “Highly Relativistic Nucleus-Nucleus Collisions: The Central Rapidity Region”, *Phys. Rev. D* **27** (1983) 140–151.
- [5] **STAR** Collaboration, J. Adams *et al.*, “Experimental and theoretical challenges in the search for the quark gluon plasma: The STAR Collaboration’s critical assessment of the evidence from RHIC collisions”, *Nucl. Phys. A* **757** (2005) 102–183, arXiv:nucl-ex/0501009.
- [6] **PHENIX** Collaboration, K. Adcox *et al.*, “Formation of dense partonic matter in relativistic nucleus-nucleus collisions at RHIC: Experimental evaluation by the PHENIX collaboration”, *Nucl. Phys. A* **757** (2005) 184–283, arXiv:nucl-ex/0410003.
- [7] B. Muller, J. Schukraft, and B. Wyslouch, “First Results from Pb+Pb collisions at the LHC”, *Ann. Rev. Nucl. Part. Sci.* **62** (2012) 361–386, arXiv:1202.3233 [hep-ex].
- [8] P. Braun-Munzinger, V. Koch, T. Schäfer, and J. Stachel, “Properties of hot and dense matter from relativistic heavy ion collisions”, *Phys. Rept.* **621** (2016) 76–126.
- [9] W. Busza, K. Rajagopal, and W. van der Schee, “Heavy Ion Collisions: The Big Picture, and the Big Questions”, *Ann. Rev. Nucl. Part. Sci.* **68** (2018) 339–376, arXiv:1802.04801 [hep-ph].
- [10] G.-Y. Qin and X.-N. Wang, “Jet quenching in high-energy heavy-ion collisions”, *Int. J. Mod. Phys. E* **24** (2015) 1530014, arXiv:1511.00790 [hep-ph].
- [11] J.-P. Blaizot and Y. Mehtar-Tani, “Jet Structure in Heavy Ion Collisions”, *Int. J. Mod. Phys. E* **24** (2015) 1530012, arXiv:1503.05958 [hep-ph].
- [12] A. Majumder and M. Van Leeuwen, “The Theory and Phenomenology of Perturbative QCD Based Jet Quenching”, *Prog. Part. Nucl. Phys.* **66** (2011) 41–92, arXiv:1002.2206 [hep-ph].
- [13] A. J. Larkoski, S. Marzani, G. Soyez, and J. Thaler, “Soft Drop”, *JHEP* **05** (2014) 146, arXiv:1402.2657 [hep-ph].
- [14] M. Dasgupta, A. Fregoso, S. Marzani, and G. P. Salam, “Towards an understanding of jet

- substructure”, *JHEP* **09** (2013) 029, arXiv:1307.0007 [hep-ph].
- [15] A. J. Larkoski, S. Marzani, and J. Thaler, “Sudakov Safety in Perturbative QCD”, *Phys. Rev.* **D91** (2015) 111501, arXiv:1502.01719 [hep-ph].
- [16] Y. Mehtar-Tani, A. Soto-Ontoso, and K. Tywoniuk, “Dynamical grooming of QCD jets”, *Phys. Rev. D* **101** (2020) 034004, arXiv:1911.00375 [hep-ph].
- [17] Y. Mehtar-Tani, A. Soto-Ontoso, and K. Tywoniuk, “Tagging boosted hadronic objects with dynamical grooming”, *Phys. Rev. D* **102** (2020) 114013, arXiv:2005.07584 [hep-ph].
- [18] P. Caucal, A. Soto-Ontoso, and A. Takacs, “Dynamical Grooming meets LHC data”, *JHEP* **07** (2021) 020, arXiv:2103.06566 [hep-ph].
- [19] P. Caucal, A. Soto-Ontoso, and A. Takacs, “Dynamically groomed jet radius in heavy-ion collisions”, *Phys. Rev. D* **105** (2022) 114046, arXiv:2111.14768 [hep-ph].
- [20] Y.-T. Chien and I. Vitev, “Probing the Hardest Branching within Jets in Heavy-Ion Collisions”, *Phys. Rev. Lett.* **119** (2017) 112301.
- [21] Y. Mehtar-Tani and K. Tywoniuk, “Groomed jets in heavy-ion collisions: sensitivity to medium-induced bremsstrahlung”, *JHEP* **04** (2017) 125, arXiv:1610.08930 [hep-ph].
- [22] N.-B. Chang, S. Cao, and G.-Y. Qin, “Probing medium-induced jet splitting and energy loss in heavy-ion collisions”, *Phys. Lett. B* **781** (2018) 423–432, arXiv:1707.03767 [hep-ph].
- [23] G. Milhano, U. A. Wiedemann, and K. C. Zapp, “Sensitivity of jet substructure to jet-induced medium response”, *Phys. Lett. B* **779** (2018) 409–413, arXiv:1707.04142 [hep-ph].
- [24] R. Kunnawalkam Elayavalli and K. C. Zapp, “Medium response in JEWEL and its impact on jet shape observables in heavy ion collisions”, *JHEP* **07** (2017) 141, arXiv:1707.01539 [hep-ph].
- [25] P. Caucal, E. Iancu, and G. Soyez, “Deciphering the z_g distribution in ultrarelativistic heavy ion collisions”, *JHEP* **10** (2019) 273, arXiv:1907.04866 [hep-ph].
- [26] F. Ringer, B.-W. Xiao, and F. Yuan, “Can we observe jet P_T -broadening in heavy-ion collisions at the LHC?”, *Phys. Lett. B* **808** (2020) 135634, arXiv:1907.12541 [hep-ph].
- [27] J. Casalderrey-Solana, G. Milhano, D. Pablos, and K. Rajagopal, “Modification of Jet Substructure in Heavy Ion Collisions as a Probe of the Resolution Length of Quark-Gluon Plasma”, *JHEP* **01** (2020) 044, arXiv:1907.11248 [hep-ph].
- [28] H. A. Andrews *et al.*, “Novel tools and observables for jet physics in heavy-ion collisions”, *J. Phys. G* **47** (2020) 065102, arXiv:1808.03689 [hep-ph].
- [29] J. Mulligan and M. Ploskon, “Identifying groomed jet splittings in heavy-ion collisions”, *Phys. Rev. C* **102** (2020) 044913, arXiv:2006.01812 [hep-ph].
- [30] ALICE Collaboration, S. Acharya *et al.*, “Measurements of the groomed and ungroomed jet angularities in pp collisions at $\sqrt{s} = 5.02$ TeV”, *JHEP* **05** (2022) 061, arXiv:2107.11303 [nucl-ex].
- [31] ALICE Collaboration, S. Acharya *et al.*, “Measurement of the groomed jet radius and momentum splitting fraction in pp and Pb–Pb collisions at $\sqrt{s_{NN}} = 5.02$ TeV”, *Phys. Rev. Lett.* **128** (2022) 102001, arXiv:2107.12984 [nucl-ex].
- [32] ATLAS Collaboration, G. Aad *et al.*, “Measurement of soft-drop jet observables in pp collisions with the ATLAS detector at $\sqrt{s} = 13$ TeV”, *Phys. Rev. D* **101** (2020) 052007, arXiv:1912.09837 [hep-ex].
- [33] CMS Collaboration, A. M. Sirunyan *et al.*, “Measurement of the Splitting Function in pp and Pb-Pb Collisions at $\sqrt{s_{NN}} = 5.02$ TeV”, *Phys. Rev. Lett.* **120** (2018) 142302, arXiv:1708.09429 [nucl-ex].
- [34] CMS Collaboration, A. M. Sirunyan *et al.*, “Measurement of jet substructure observables in $t\bar{t}$ events from proton-proton collisions at $\sqrt{s} = 13$ TeV”, *Phys. Rev. D* **98** (2018) 092014, arXiv:1808.07340 [hep-ex].

- [35] **CMS** Collaboration, A. M. Sirunyan *et al.*, “Measurement of the groomed jet mass in PbPb and pp collisions at $\sqrt{s_{NN}} = 5.02$ TeV”, *JHEP* **10** (2018) 161, arXiv:1805.05145 [hep-ex].
- [36] **STAR** Collaboration, J. Adam *et al.*, “Measurement of groomed jet substructure observables in p+p collisions at $\sqrt{s} = 200$ GeV with STAR”, *Phys. Lett. B* **811** (2020) 135846, arXiv:2003.02114 [hep-ex].
- [37] **STAR** Collaboration, M. S. Abdallah *et al.*, “Differential measurements of jet substructure and partonic energy loss in Au+Au collisions at $\sqrt{s_{NN}} = 200$ GeV”, *Phys. Rev. C* **105** (2022) 044906, arXiv:2109.09793 [nucl-ex].
- [38] Y. Chen *et al.*, “Jet energy spectrum and substructure in e^+e^- collisions at 91.2 GeV with ALEPH Archived Data”, *JHEP* **06** (2022) 008, arXiv:2111.09914 [hep-ex].
- [39] F. A. Dreyer, G. P. Salam, and G. Soyez, “The Lund Jet Plane”, *JHEP* **12** (2018) 064, arXiv:1807.04758 [hep-ph].
- [40] Z.-B. Kang, K. Lee, X. Liu, D. Neill, and F. Ringer, “The soft drop groomed jet radius at NLL”, *JHEP* **2** (2020) 054, arXiv:1908.01783 [hep-ph].
- [41] P. Cal, K. Lee, F. Ringer, and W. J. Waalewijn, “The soft drop momentum sharing fraction z_g beyond leading-logarithmic accuracy”, *Phys. Lett. B* **833** (2022) 137390, arXiv:2106.04589 [hep-ph].
- [42] T. Sjöstrand, S. Ask, J. R. Christiansen, R. Corke, N. Desai, P. Ilten, S. Mrenna, S. Prestel, C. O. Rasmussen, and P. Z. Skands, “An introduction to PYTHIA 8.2”, *Comput. Phys. Commun.* **191** (2015) 159–177, arXiv:1410.3012 [hep-ph].
- [43] P. Skands, S. Carrazza, and J. Rojo, “Tuning PYTHIA 8.1: the Monash 2013 Tune”, *Eur. Phys. J. C* **74** (2014) 3024, arXiv:1404.5630 [hep-ph].
- [44] H.-M. Chang, M. Procura, J. Thaler, and W. J. Waalewijn, “Calculating Track-Based Observables for the LHC”, *Phys. Rev. Lett.* **111** (2013) 102002, arXiv:1303.6637 [hep-ph].
- [45] H. Chen, I. Moutl, X. Zhang, and H. X. Zhu, “Rethinking jets with energy correlators: Tracks, resummation, and analytic continuation”, *Phys. Rev. D* **102** (2020) 054012, arXiv:2004.11381 [hep-ph].
- [46] Y.-T. Chien, R. Rahn, S. Schrijnder van Velzen, D. Y. Shao, W. J. Waalewijn, and B. Wu, “Recoil-free azimuthal angle for precision boson-jet correlation”, *Phys. Lett. B* **815** (2021) 136124, arXiv:2005.12279 [hep-ph].
- [47] **ALICE** Collaboration, K. Aamodt *et al.*, “The ALICE experiment at the CERN LHC”, *JINST* **3** (2008) S08002.
- [48] **ALICE** Collaboration, B. B. Abelev *et al.*, “Performance of the ALICE Experiment at the CERN LHC”, *Int. J. Mod. Phys. A* **29** (2014) 1430044, arXiv:1402.4476 [nucl-ex].
- [49] **ALICE** Collaboration, E. Abbas *et al.*, “Performance of the ALICE VZERO system”, *JINST* **8** (2013) P10016, arXiv:1306.3130 [nucl-ex].
- [50] **ALICE** Collaboration, S. Acharya *et al.*, “Measurements of inclusive jet spectra in pp and central Pb–Pb collisions at $\sqrt{s_{NN}} = 5.02$ TeV”, *Phys. Rev. C* **101** (2020) 034911, arXiv:1909.09718 [nucl-ex].
- [51] **ALICE** Collaboration, S. Acharya *et al.*, “ALICE 2017 luminosity determination for pp collisions at $\sqrt{s} = 5$ TeV”, *ALICE-PUBLIC-2018-014*. <http://cds.cern.ch/record/2648933>.
- [52] J. Alme and et al., “The ALICE TPC, a large 3-dimensional tracking device with fast readout for ultra-high multiplicity events”, *Nucl. Instrum. Meth. A: Accelerators, Spectrometers, Detectors and Associated Equipment* **622** (2010) 316–367.
- [53] **ALICE** Collaboration, K. Aamodt *et al.*, “Alignment of the ALICE Inner Tracking System with cosmic-ray tracks”, *JINST* **5** (2010) P03003, arXiv:1001.0502 [physics.ins-det].
- [54] R. Brun, F. Bruyant, M. Maire, A. C. McPherson, and P. Zancarini, *GEANT 3: user’s guide Geant*

- 3.10, *Geant 3.11; rev. version*. CERN, Geneva, 1987. <https://cds.cern.ch/record/1119728>.
- [55] M. Cacciari, G. P. Salam, and G. Soyez, “FastJet User Manual”, *Eur. Phys. J. C* **72** (2012) 1896.
- [56] M. Cacciari, G. P. Salam, and G. Soyez, “The anti- k_t jet clustering algorithm”, *JHEP* **04** (2008) 063, [arXiv:0802.1189](https://arxiv.org/abs/0802.1189) [hep-ph].
- [57] M. Cacciari, G. P. Salam, and G. Soyez, “The Catchment Area of Jets”, *JHEP* **04** (2008) 005, [arXiv:0802.1188](https://arxiv.org/abs/0802.1188) [hep-ph].
- [58] ALICE Collaboration, S. Acharya *et al.*, “The ALICE definition of primary particles”, *ALICE-PUBLIC-2017-005*. <https://cds.cern.ch/record/2270008>.
- [59] G. D’Agostini, “A multidimensional unfolding method based on bayes’ theorem”, *Nucl. Instrum. Meth. A: Accelerators, Spectrometers, Detectors and Associated Equipment* **362** (1995) 487 – 498.
- [60] G. D’Agostini, “Improved iterative Bayesian unfolding”, [arXiv:1010.0632](https://arxiv.org/abs/1010.0632) [physics.data-an].
- [61] “RooUnfold.” <http://hepunix.rl.ac.uk/~adye/software/unfold/RooUnfold.html>. Access date: May 31 2020.
- [62] J. Bellm *et al.*, “Herwig 7.0/Herwig++ 3.0 release note”, *Eur. Phys. J. C* **76** (2016) 196, [arXiv:1512.01178](https://arxiv.org/abs/1512.01178) [hep-ph].
- [63] G. Altarelli and G. Parisi, “Asymptotic Freedom in Parton Language”, *Nucl. Phys. B* **126** (1977) 298–318.
- [64] C. W. Bauer, D. Pirjol, and I. W. Stewart, “Soft collinear factorization in effective field theory”, *Phys. Rev. D* **65** (2002) 054022, [arXiv:hep-ph/0109045](https://arxiv.org/abs/hep-ph/0109045).

A The ALICE Collaboration

S. Acharya ^{124,131}, D. Adamová ⁸⁶, A. Adler⁶⁹, G. Aglieri Rinella ³², M. Agnello ²⁹, N. Agrawal ⁵⁰, Z. Ahammed ¹³¹, S. Ahmad ¹⁵, S.U. Ahn ⁷⁰, I. Ahuja ³⁷, A. Akindinov ¹³⁹, M. Al-Turany ⁹⁸, D. Aleksandrov ¹³⁹, B. Alessandro ⁵⁵, H.M. Alfanda ⁶, R. Alfaro Molina ⁶⁶, B. Ali ¹⁵, Y. Ali¹³, A. Alici ²⁵, N. Alizadehvandchali ¹¹³, A. Alkin ³², J. Alme ²⁰, G. Alocco ⁵¹, T. Alt ⁶³, I. Altsybeev ¹³⁹, M.N. Anaam ⁶, C. Andrei ⁴⁵, A. Andronic ¹³⁴, V. Angelov ⁹⁵, F. Antinori ⁵³, P. Antonioli ⁵⁰, C. Anuj ¹⁵, N. Apadula ⁷⁴, L. Aphecetche ¹⁰³, H. Appelshäuser ⁶³, S. Arcelli ²⁵, R. Arnaldi ⁵⁵, I.C. Arsene ¹⁹, M. Arslanok ¹³⁶, A. Augustinus ³², R. Averbeck ⁹⁸, S. Aziz ⁷², M.D. Azmi ¹⁵, A. Badalà ⁵², Y.W. Baek ⁴⁰, X. Bai ⁹⁸, R. Bailhache ⁶³, Y. Bailung ⁴⁷, R. Bala ⁹¹, A. Balbino ²⁹, A. Baldisseri ¹²⁷, B. Balis ², D. Banerjee ⁴, Z. Banoo ⁹¹, R. Barbera ²⁶, L. Barioglio ⁹⁶, M. Barlou⁷⁸, G.G. Barnaföldi ¹³⁵, L.S. Barnby ⁸⁵, V. Barret ¹²⁴, L. Barreto ¹⁰⁹, C. Bartels ¹¹⁶, K. Barth ³², E. Bartsch ⁶³, F. Baruffaldi ²⁷, N. Bastid ¹²⁴, S. Basu ⁷⁵, G. Batigne ¹⁰³, D. Battistini ⁹⁶, B. Batyunya ¹⁴⁰, D. Bauri⁴⁶, J.L. Bazo Alba ¹⁰¹, I.G. Bearden ⁸³, C. Beattie ¹³⁶, P. Becht ⁹⁸, D. Behera ⁴⁷, I. Belikov ¹²⁶, A.D.C. Bell Hechavarria ¹³⁴, F. Bellini ²⁵, R. Bellwied ¹¹³, S. Belokurova ¹³⁹, V. Belyaev ¹³⁹, G. Bencedi ^{135,64}, S. Beole ²⁴, A. Bercuci ⁴⁵, Y. Berdnikov ¹³⁹, A. Berdnikova ⁹⁵, L. Bergmann ⁹⁵, M.G. Besoiu ⁶², L. Betev ³², P.P. Bhaduri ¹³¹, A. Bhasin ⁹¹, I.R. Bhat⁹¹, M.A. Bhat ⁴, B. Bhattacharjee ⁴¹, L. Bianchi ²⁴, N. Bianchi ⁴⁸, J. Bielčik ³⁵, J. Bielčíková ⁸⁶, J. Biernat ¹⁰⁶, A. Bilandzic ⁹⁶, G. Biro ¹³⁵, S. Biswas ⁴, J.T. Blair ¹⁰⁷, D. Blau ¹³⁹, M.B. Blidaru ⁹⁸, N. Bluhme³⁸, C. Blume ⁶³, G. Boca ^{21,54}, F. Bock ⁸⁷, T. Bodova ²⁰, A. Bogdanov¹³⁹, S. Boi ²², J. Bok ⁵⁷, L. Boldizsár ¹³⁵, A. Bolozdynya ¹³⁹, M. Bombara ³⁷, P.M. Bond ³², G. Bonomi ^{130,54}, H. Borel ¹²⁷, A. Borissov ¹³⁹, H. Bossi ¹³⁶, E. Botta ²⁴, L. Bratrud ⁶³, P. Braun-Munzinger ⁹⁸, M. Bregant ¹⁰⁹, M. Broz ³⁵, G.E. Bruno ^{97,31}, M.D. Buckland ¹¹⁶, D. Budnikov ¹³⁹, H. Buesching ⁶³, S. Bufalino ²⁹, O. Bugnon¹⁰³, P. Buhler ¹⁰², Z. Buthelezi ^{67,120}, J.B. Butt¹³, A. Bylinkin ¹¹⁵, S.A. Bysiak¹⁰⁶, M. Cai ^{27,6}, H. Caines ¹³⁶, A. Caliva ⁹⁸, E. Calvo Villar ¹⁰¹, J.M.M. Camacho ¹⁰⁸, R.S. Camacho⁴⁴, P. Camerini ²³, F.D.M. Canedo ¹⁰⁹, M. Carabas ¹²³, F. Carnesecchi ³², R. Caron ^{125,127}, J. Castillo Castellanos ¹²⁷, F. Catalano ²⁹, C. Ceballos Sanchez ¹⁴⁰, I. Chakaberia ⁷⁴, P. Chakraborty ⁴⁶, S. Chandra ¹³¹, S. Chapeland ³², M. Chartier ¹¹⁶, S. Chattopadhyay ¹³¹, S. Chattopadhyay ⁹⁹, T.G. Chavez ⁴⁴, T. Cheng ⁶, C. Cheshkov ¹²⁵, B. Cheynis ¹²⁵, V. Chibante Barroso ³², D.D. Chinellato ¹¹⁰, E.S. Chizzali ^{11,96}, J. Cho ⁵⁷, S. Cho ⁵⁷, P. Chochula ³², P. Christakoglou ⁸⁴, C.H. Christensen ⁸³, P. Christiansen ⁷⁵, T. Chujo ¹²², M. Ciaccio ²⁹, C. Cicalo ⁵¹, L. Cifarelli ²⁵, F. Cindolo ⁵⁰, M.R. Ciupek⁹⁸, G. Clai^{III,50}, F. Colamaria ⁴⁹, J.S. Colburn¹⁰⁰, D. Colella ^{97,31}, A. Collu⁷⁴, M. Colocci ³², M. Concas ^{IV,55}, G. Conesa Balbastre ⁷³, Z. Conesa del Valle ⁷², G. Contin ²³, J.G. Contreras ³⁵, M.L. Coquet ¹²⁷, T.M. Cormier^{I,87}, P. Cortese ^{129,55}, M.R. Cosentino ¹¹¹, F. Costa ³², S. Costanza ^{21,54}, P. Crochet ¹²⁴, R. Cruz-Torres ⁷⁴, E. Cuautele⁶⁴, P. Cui ⁶, L. Cunqueiro⁸⁷, A. Dainese ⁵³, M.C. Danisch ⁹⁵, A. Danu ⁶², P. Das ⁸⁰, P. Das ⁴, S. Das ⁴, S. Dash ⁴⁶, A. De Caro ²⁸, G. de Cataldo ⁴⁹, L. De Cilladi ²⁴, J. de Cuveland³⁸, A. De Falco ²², D. De Gruttola ²⁸, N. De Marco ⁵⁵, C. De Martin ²³, S. De Pasquale ²⁸, S. Deb ⁴⁷, H.F. Degenhardt¹⁰⁹, K.R. Deja ¹³², R. Del Grande ⁹⁶, L. Dello Stritto ²⁸, W. Deng ⁶, P. Dhankher ¹⁸, D. Di Bari ³¹, A. Di Mauro ³², R.A. Diaz ^{140,7}, T. Dietel ¹¹², Y. Ding ^{125,6}, R. Divià ³², D.U. Dixit ¹⁸, Ø. Djuvsland²⁰, U. Dmitrieva ¹³⁹, A. Dobrin ⁶², B. Dönigus ⁶³, A.K. Dubey ¹³¹, J.M. Dubinski¹³², A. Dubla ⁹⁸, S. Dudi ⁹⁰, P. Dupieux ¹²⁴, M. Durkac¹⁰⁵, N. Dzalaiova¹², T.M. Eder ¹³⁴, R.J. Ehlers ⁸⁷, V.N. Eikeland²⁰, F. Eisenhut ⁶³, D. Elia ⁴⁹, B. Erasmus ¹⁰³, F. Ercolessi ²⁵, F. Erhardt ⁸⁹, M.R. Ersdal²⁰, B. Espagnon ⁷², G. Eulisse ³², D. Evans ¹⁰⁰, S. Evdokimov ¹³⁹, L. Fabbietti ⁹⁶, M. Faggin ²⁷, J. Faivre ²⁷, F. Fan ⁶, W. Fan ⁷⁴, A. Fantoni ⁴⁸, M. Fasel ⁸⁷, P. Fedchio²⁹, A. Feliciello ⁵⁵, G. Feofilov ¹³⁹, A. Fernández Téllez ⁴⁴, M.B. Ferrer ³², A. Ferrero ¹²⁷, A. Ferretti ²⁴, V.J.G. Feuillard ⁹⁵, J. Figiel ¹⁰⁶, V. Filova³⁵, D. Finogeev ¹³⁹, F.M. Fionda ⁵¹, G. Fiorenza⁹⁷, F. Flor ¹¹³, A.N. Flores ¹⁰⁷, S. Foertsch ⁶⁷, I. Fokin ⁹⁵, S. Fokin ¹³⁹, E. Fragiaco ⁵⁶, E. Frajna ¹³⁵, U. Fuchs ³², N. Funicello ²⁸, C. Furget ⁷³, A. Furs ¹³⁹, J.J. Gaardhøje ⁸³, M. Gagliardi ²⁴, A.M. Gago ¹⁰¹, A. Gal¹²⁶, C.D. Galvan ¹⁰⁸, P. Ganoti ⁷⁸, C. Garabatos ⁹⁸, J.R.A. Garcia ⁴⁴, E. Garcia-Solis ⁹, K. Garg ¹⁰³, C. Gargiulo ³², A. Garibli⁸¹, K. Garner¹³⁴, E.F. Gauger ¹⁰⁷, A. Gautam ¹¹⁵, M.B. Gay Ducati ⁶⁵, M. Germain ¹⁰³, S.K. Ghosh⁴, M. Giacalone ²⁵, P. Gianotti ⁴⁸, P. Giubellino ^{98,55}, P. Giubilato ²⁷, A.M.C. Glaenger ¹²⁷, P. Glässel ⁹⁵, E. Glimos¹¹⁹, D.J.Q. Goh⁷⁶, V. Gonzalez ¹³³, L.H. González-Trueba ⁶⁶, S. Gorbunov³⁸, M. Gorgon ², L. Görlich ¹⁰⁶, S. Gotovac³³, V. Grabski ⁶⁶, L.K. Graczykowski ¹³², E. Grecka ⁸⁶, L. Greiner ⁷⁴, A. Grelli ⁵⁸, C. Grigoras ³², V. Grigoriev ¹³⁹, S. Grigoryan ^{140,1}, F. Grosa ³², J.F. Grosse-Oetringhaus ³², R. Grosso ⁹⁸, D. Grund ³⁵, G.G. Guardiano ¹¹⁰, R. Guernane ⁷³, M. Guilbaud ¹⁰³, K. Gulbrandsen ⁸³, T. Gunji ¹²¹, W. Guo ⁶, A. Gupta ⁹¹, R. Gupta ⁹¹,

S.P. Guzman ⁴⁴, L. Gyulai ¹³⁵, M.K. Habib ⁹⁸, C. Hadjidakis ⁷², H. Hamagaki ⁷⁶, M. Hamid ⁶, Y. Han ¹³⁷, R. Hannigan ¹⁰⁷, M.R. Haque ¹³², A. Harlenderova ⁹⁸, J.W. Harris ¹³⁶, A. Harton ⁹, J.A. Hasenbichler ³², H. Hassan ⁸⁷, D. Hatzifotiadou ⁵⁰, P. Hauer ⁴², L.B. Havener ¹³⁶, S.T. Heckel ⁹⁶, E. Hellbär ⁹⁸, H. Helstrup ³⁴, T. Herman ³⁵, G. Herrera Corral ⁸, F. Herrmann ¹³⁴, K.F. Hetland ³⁴, B. Heybeck ⁶³, H. Hillemanns ³², C. Hills ¹¹⁶, B. Hippolyte ¹²⁶, B. Hofman ⁵⁸, B. Hohlweger ⁸⁴, J. Honeremann ¹³⁴, G.H. Hong ¹³⁷, D. Horak ³⁵, A. Horzyk ², R. Hosokawa ¹⁴, Y. Hou ⁶, P. Hristov ³², C. Hughes ¹¹⁹, P. Huhn ⁶³, L.M. Huhta ¹¹⁴, C.V. Hulse ⁷², T.J. Humanic ⁸⁸, H. Hushnud ⁹⁹, A. Hutson ¹¹³, D. Hutter ³⁸, J.P. Iddon ¹¹⁶, R. Ilkaev ¹³⁹, H. Ilyas ¹³, M. Inaba ¹²², G.M. Innocenti ³², M. Ippolitov ¹³⁹, A. Isakov ⁸⁶, T. Isidori ¹¹⁵, M.S. Islam ⁹⁹, M. Ivanov ⁹⁸, V. Ivanov ¹³⁹, V. Izucheev ¹³⁹, M. Jablonski ², B. Jacak ⁷⁴, N. Jacazio ³², P.M. Jacobs ⁷⁴, S. Jadlovská ¹⁰⁵, J. Jadlovsky ¹⁰⁵, L. Jaffe ³⁸, C. Jahnke ¹¹⁰, M.A. Janik ¹³², T. Janson ⁶⁹, M. Jercic ⁸⁹, O. Jevons ¹⁰⁰, A.A.P. Jimenez ⁶⁴, F. Jonas ^{87,134}, P.G. Jones ¹⁰⁰, J.M. Jowett ^{32,98}, J. Jung ⁶³, M. Jung ⁶³, A. Junique ³², A. Jusko ¹⁰⁰, M.J. Kabus ^{32,132}, J. Kaewjai ¹⁰⁴, P. Kalinak ⁵⁹, A.S. Kalteyer ⁹⁸, A. Kalweit ³², V. Kaplin ¹³⁹, A. Karasu Uysal ⁷¹, D. Karatovic ⁸⁹, O. Karavichev ¹³⁹, T. Karavicheva ¹³⁹, P. Karczmarczyk ¹³², E. Karpechev ¹³⁹, V. Kashyap ⁸⁰, A. Kazantsev ¹³⁹, U. Keschull ⁶⁹, R. Keidel ¹³⁸, D.L.D. Keijdener ⁵⁸, M. Keil ³², B. Ketzer ⁴², A.M. Khan ⁶, S. Khan ¹⁵, A. Khanzadeev ¹³⁹, Y. Kharlov ¹³⁹, A. Khatun ¹⁵, A. Khuntia ¹⁰⁶, B. Kileng ³⁴, B. Kim ¹⁶, C. Kim ¹⁶, D.J. Kim ¹¹⁴, E.J. Kim ⁶⁸, J. Kim ¹³⁷, J.S. Kim ⁴⁰, J. Kim ⁹⁵, J. Kim ⁶⁸, M. Kim ⁹⁵, S. Kim ¹⁷, T. Kim ¹³⁷, S. Kirsch ⁶³, I. Kisel ³⁸, S. Kiselev ¹³⁹, A. Kisiel ¹³², J.P. Kitowski ², J.L. Klay ⁵, J. Klein ³², S. Klein ⁷⁴, C. Klein-Bösing ¹³⁴, M. Kleiner ⁶³, T. Klemenz ⁹⁶, A. Kluge ³², A.G. Knospe ¹¹³, C. Kobdaj ¹⁰⁴, T. Kollegger ⁹⁸, A. Kondratyev ¹⁴⁰, N. Kondratyeva ¹³⁹, E. Kondratyuk ¹³⁹, J. Konig ⁶³, S.A. Konigstorfer ⁹⁶, P.J. Konopka ³², G. Kornakov ¹³², S.D. Koryciak ², A. Kotliarov ⁸⁶, O. Kovalenko ⁷⁹, V. Kovalenko ¹³⁹, M. Kowalski ¹⁰⁶, I. Králik ⁵⁹, A. Kravčáková ³⁷, L. Kreis ⁹⁸, M. Krivda ^{100,59}, F. Krizek ⁸⁶, K. Krizkova Gajdosova ³⁵, M. Kroesen ⁹⁵, M. Krüger ⁶³, D.M. Krupova ³⁵, E. Kryshen ¹³⁹, M. Krzewicki ³⁸, V. Kučera ³², C. Kuhn ¹²⁶, P.G. Kuijer ⁸⁴, T. Kumaoka ¹²², D. Kumar ¹³¹, L. Kumar ⁹⁰, N. Kumar ⁹⁰, S. Kundu ³², P. Kurashvili ⁷⁹, A. Kurepin ¹³⁹, A.B. Kurepin ¹³⁹, S. Kushpil ⁸⁶, J. Kvapil ¹⁰⁰, M.J. Kweon ⁵⁷, J.Y. Kwon ⁵⁷, Y. Kwon ¹³⁷, S.L. La Pointe ³⁸, P. La Rocca ²⁶, Y.S. Lai ⁷⁴, A. Lakrathok ¹⁰⁴, M. Lamanna ³², R. Langoy ¹¹⁸, P. Larionov ⁴⁸, E. Laudi ³², L. Lautner ^{32,96}, R. Lavicka ¹⁰², T. Lazareva ¹³⁹, R. Lea ^{130,54}, J. Leibrach ³⁸, R.C. Lemmon ⁸⁵, I. León Monzón ¹⁰⁸, M.M. Lesch ⁹⁶, E.D. Lesser ¹⁸, M. Lettrich ⁹⁶, P. Lévai ¹³⁵, X. Li ¹⁰, X.L. Li ⁶, J. Lien ¹¹⁸, R. Lietava ¹⁰⁰, B. Lim ¹⁶, S.H. Lim ¹⁶, V. Lindenstruth ³⁸, A. Lindner ⁴⁵, C. Lippmann ⁹⁸, A. Liu ¹⁸, D.H. Liu ⁶, J. Liu ¹¹⁶, I.M. Lofnes ²⁰, V. Loginov ¹³⁹, C. Loizides ⁸⁷, P. Loncar ³³, J.A. Lopez ⁹⁵, X. Lopez ¹²⁴, E. López Torres ⁷, P. Lu ^{98,117}, J.R. Luhder ¹³⁴, M. Lunardon ²⁷, G. Luparello ⁵⁶, Y.G. Ma ³⁹, A. Maevskaya ¹³⁹, M. Mager ³², T. Mahmoud ⁴², A. Maire ¹²⁶, M. Malaev ¹³⁹, N.M. Malik ⁹¹, Q.W. Malik ¹⁹, S.K. Malik ⁹¹, L. Malinina ^{VII,140}, D. Mal'Kevich ¹³⁹, D. Mallick ⁸⁰, N. Mallick ⁴⁷, G. Mandaglio ^{30,52}, V. Manko ¹³⁹, F. Manso ¹²⁴, V. Manzari ⁴⁹, Y. Mao ⁶, G.V. Margagliotti ²³, A. Margotti ⁵⁰, A. Marín ⁹⁸, C. Markert ¹⁰⁷, M. Marquard ⁶³, N.A. Martin ⁹⁵, P. Martinengo ³², J.L. Martinez ¹¹³, M.I. Martínez ⁴⁴, G. Martínez García ¹⁰³, S. Masciocchi ⁹⁸, M. Masera ²⁴, A. Masoni ⁵¹, L. Massacrier ⁷², A. Mastroserio ^{128,49}, A.M. Mathis ⁹⁶, O. Matonoha ⁷⁵, P.F.T. Matuoka ¹⁰⁹, A. Matyja ¹⁰⁶, C. Mayer ¹⁰⁶, A.L. Mazuecos ³², F. Mazzaschi ²⁴, M. Mazzilli ³², J.E. Mdhuli ¹²⁰, A.F. Mechler ⁶³, Y. Melikyan ¹³⁹, A. Menchaca-Rocha ⁶⁶, E. Meninno ^{102,28}, A.S. Menon ¹¹³, M. Meres ¹², S. Mhlanga ^{112,67}, Y. Miake ¹²², L. Micheletti ⁵⁵, L.C. Migliorin ¹²⁵, D.L. Mihaylov ⁹⁶, K. Mikhaylov ^{140,139}, A.N. Mishra ¹³⁵, D. Miśkowiec ⁹⁸, A. Modak ⁴, A.P. Mohanty ⁵⁸, B. Mohanty ⁸⁰, M. Mohisin Khan ^{V,15}, M.A. Molander ⁴³, Z. Moravcova ⁸³, C. Mordasini ⁹⁶, D.A. Moreira De Godoy ¹³⁴, I. Morozov ¹³⁹, A. Morsch ³², T. Mrnjavac ³², V. Muccifora ⁴⁸, E. Mudnic ³³, S. Muhuri ¹³¹, J.D. Mulligan ⁷⁴, A. Mulliri ²², M.G. Munhoz ¹⁰⁹, R.H. Munzer ⁶³, H. Murakami ¹²¹, S. Murray ¹¹², L. Musa ³², J. Musinsky ⁵⁹, J.W. Myrcha ¹³², B. Naik ¹²⁰, R. Nair ⁷⁹, B.K. Nandi ⁴⁶, R. Nania ⁵⁰, E. Nappi ⁴⁹, A.F. Nassirpour ⁷⁵, A. Nath ⁹⁵, C. Nattrass ¹¹⁹, A. Neagu ¹⁹, A. Negru ¹²³, L. Nellen ⁶⁴, S.V. Nesbo ³⁴, G. Neskovic ³⁸, D. Nesterov ¹³⁹, B.S. Nielsen ⁸³, E.G. Nielsen ⁸³, S. Nikolaev ¹³⁹, S. Nikulin ¹³⁹, V. Nikulin ¹³⁹, F. Noferini ⁵⁰, S. Noh ¹¹, P. Nomokonov ¹⁴⁰, J. Norman ¹¹⁶, N. Novitzky ¹²², P. Nowakowski ¹³², A. Nyanin ¹³⁹, J. Nystrand ²⁰, M. Ogino ⁷⁶, A. Ohlson ⁷⁵, V.A. Okorokov ¹³⁹, J. Olienczak ¹³², A.C. Oliveira Da Silva ¹¹⁹, M.H. Oliver ¹³⁶, A. Onnerstad ¹¹⁴, C. Oppedisano ⁵⁵, A. Ortiz Velasquez ⁶⁴, A. Oskarsson ⁷⁵, J. Otwinowski ¹⁰⁶, M. Oya ⁹³, K. Oyama ⁷⁶, Y. Pachmayer ⁹⁵, S. Padhan ⁴⁶, D. Pagano ^{130,54}, G. Paic ⁶⁴, A. Palasciano ⁴⁹, S. Panebianco ¹²⁷, J. Park ⁵⁷, J.E. Parkkila ^{32,114}, S.P. Pathak ¹¹³, R.N. Patra ⁹¹, B. Paul ²², H. Pei ⁶, T. Peitzmann ⁵⁸, X. Peng ⁶, L.G. Pereira ⁶⁵, H. Pereira Da Costa ¹²⁷, D. Peresunko ¹³⁹, G.M. Perez ⁷, S. Perrin ¹²⁷, Y. Pestov ¹³⁹,

V. Petráček³⁵, V. Petrov¹³⁹, M. Petrovici⁴⁵, R.P. Pezzi^{103,65}, S. Piano⁵⁶, M. Pikna¹², P. Pillot¹⁰³, O. Pinazza^{50,32}, L. Pinsky¹¹³, C. Pinto^{96,26}, S. Pisano⁴⁸, M. Płoskoń⁷⁴, M. Planinic⁸⁹, F. Pliquett⁶³, M.G. Poghosyan⁸⁷, S. Politano²⁹, N. Poljak⁸⁹, A. Pop⁴⁵, S. Porteboeuf-Houssais¹²⁴, J. Porter⁷⁴, V. Pozdniakov¹⁴⁰, S.K. Prasad⁴, S. Prasad⁴⁷, R. Preghenella⁵⁰, F. Prino⁵⁵, C.A. Pruneau¹³³, I. Pshenichnov¹³⁹, M. Puccio³², S. Qiu⁸⁴, L. Quaglia²⁴, R.E. Quishpe¹¹³, S. Ragoni¹⁰⁰, A. Rakotozafindrabe¹²⁷, L. Ramello^{129,55}, F. Rami¹²⁶, S.A.R. Ramirez⁴⁴, T.A. Rancien⁷³, R. Raniwala⁹², S. Raniwala⁹², S.S. Räsänen⁴³, R. Rath⁴⁷, I. Ravasenga⁸⁴, K.F. Read^{87,119}, A.R. Redelbach³⁸, K. Redlich^{VI,79}, A. Rehman²⁰, P. Reichelt⁶³, F. Reidt³², H.A. Reme-Ness³⁴, Z. Rescakova³⁷, K. Reygers⁹⁵, A. Riabov¹³⁹, V. Riabov¹³⁹, R. Ricci²⁸, T. Richert⁷⁵, M. Richter¹⁹, W. Riegler³², F. Riggi²⁶, C. Ristea⁶², M. Rodríguez Cahuantzi⁴⁴, K. Røed¹⁹, R. Rogalev¹³⁹, E. Rogochaya¹⁴⁰, T.S. Rogoschinski⁶³, D. Rohr³², D. Röhrich²⁰, P.F. Rojas⁴⁴, S. Rojas Torres³⁵, P.S. Rokita¹³², F. Ronchetti⁴⁸, A. Rosano^{30,52}, E.D. Rosas⁶⁴, A. Rossi⁵³, A. Roy⁴⁷, P. Roy⁹⁹, S. Roy⁴⁶, N. Rubini²⁵, O.V. Rueda⁷⁵, D. Ruggiano¹³², R. Rui²³, B. Rumyantsev¹⁴⁰, P.G. Russek², R. Russo⁸⁴, A. Rustamov⁸¹, E. Ryabinkin¹³⁹, Y. Ryabov¹³⁹, A. Rybicki¹⁰⁶, H. Rytkonen¹¹⁴, W. Rzesza¹³², O.A.M. Saarimäki⁴³, R. Sadek¹⁰³, S. Sadovsky¹³⁹, J. Saetre²⁰, K. Šafařík³⁵, S.K. Saha¹³¹, S. Saha⁸⁰, B. Sahoo⁴⁶, P. Sahoo⁴⁶, R. Sahoo⁴⁷, S. Sahoo⁶⁰, D. Sahu⁴⁷, P.K. Sahu⁶⁰, J. Saini¹³¹, K. Sajdakova³⁷, S. Sakai¹²², M.P. Salvan⁹⁸, S. Sambyal⁹¹, T.B. Saramela¹⁰⁹, D. Sarkar¹³³, N. Sarkar¹³¹, P. Sarma⁴¹, V. Sarritzu²², V.M. Sarti⁹⁶, M.H.P. Sas¹³⁶, J. Schambach⁸⁷, H.S. Scheid⁶³, C. Schiaua⁴⁵, R. Schicker⁹⁵, A. Schmah⁹⁵, C. Schmidt⁹⁸, H.R. Schmidt⁹⁴, M.O. Schmidt³², M. Schmidt⁹⁴, N.V. Schmidt^{87,63}, A.R. Schmier¹¹⁹, R. Schotter¹²⁶, J. Schukraft³², K. Schwarz⁹⁸, K. Schweda⁹⁸, G. Scioli²⁵, E. Scomparin⁵⁵, J.E. Seger¹⁴, Y. Sekiguchi¹²¹, D. Sekihata¹²¹, I. Selyuzhenkov^{98,139}, S. Senyukov¹²⁶, J.J. Seo⁵⁷, D. Serebryakov¹³⁹, L. Šerkšnytė⁹⁶, A. Sevcenco⁶², T.J. Shaba⁶⁷, A. Shabanov¹³⁹, A. Shabetai¹⁰³, R. Shahoyan³², W. Shaikh⁹⁹, A. Shangaraev¹³⁹, A. Sharma⁹⁰, D. Sharma⁴⁶, H. Sharma¹⁰⁶, M. Sharma⁹¹, N. Sharma⁹⁰, S. Sharma⁹¹, U. Sharma⁹¹, A. Shatat⁷², O. Sheibani¹¹³, K. Shigaki⁹³, M. Shimomura⁷⁷, S. Shirinkin¹³⁹, Q. Shou³⁹, Y. Sibiriak¹³⁹, S. Siddhanta⁵¹, T. Siemiarczuk⁷⁹, T.F. Silva¹⁰⁹, D. Silvermyr⁷⁵, T. Simantathammakul¹⁰⁴, R. Simeonov³⁶, G. Simonetti³², B. Singh⁹¹, B. Singh⁹⁶, R. Singh⁸⁰, R. Singh⁹¹, R. Singh⁴⁷, V.K. Singh¹³¹, V. Singhal¹³¹, T. Sinha⁹⁹, B. Sitar¹², M. Sitta^{129,55}, T.B. Skaali¹⁹, G. Skorodumovs⁹⁵, M. Slupecki⁴³, N. Smirnov¹³⁶, R.J.M. Snellings⁵⁸, E.H. Solheim¹⁹, C. Soncco¹⁰¹, J. Song¹¹³, A. Songmoolnak¹⁰⁴, F. Soramel²⁷, S. Sorensen¹¹⁹, R. Spijkers⁸⁴, I. Sputowska¹⁰⁶, J. Staa⁷⁵, J. Stachel⁹⁵, I. Stan⁶², P.J. Steffanic¹¹⁹, S.F. Stiefelmaier⁹⁵, D. Stocco¹⁰³, I. Storehaug¹⁹, M.M. Storetvedt³⁴, P. Stratmann¹³⁴, S. Strazzi²⁵, C.P. Stylianidis⁸⁴, A.A.P. Suaide¹⁰⁹, C. Suire⁷², M. Sukhanov¹³⁹, M. Suljic³², V. Sumberia⁹¹, S. Sumowidagdo⁸², S. Swain⁶⁰, A. Szabo¹², I. Szarka¹², U. Tabassam¹³, S.F. Taghavi⁹⁶, G. Tallepied^{98,124}, J. Takahashi¹¹⁰, G.J. Tambave²⁰, S. Tang^{124,6}, Z. Tang¹¹⁷, J.D. Tapia Takaki¹¹⁵, N. Tapus¹²³, L.A. Tarasovicova¹³⁴, M.G. Tarzila⁴⁵, A. Tauro³², A. Telesca³², L. Terlizzi²⁴, C. Terrevoli¹¹³, G. Tersimonov³, S. Thakur¹³¹, D. Thomas¹⁰⁷, R. Tieulent¹²⁵, A. Tikhonov¹³⁹, A.R. Timmins¹¹³, M. Tkacik¹⁰⁵, T. Tkacik¹⁰⁵, A. Toia⁶³, N. Topilskaya¹³⁹, M. Toppi⁴⁸, F. Torres-Acosta¹⁸, T. Tork⁷², A.G. Torres Ramos³¹, A. Trifiró^{30,52}, A.S. Triolo^{30,52}, S. Tripathy⁵⁰, T. Tripathy⁴⁶, S. Trogolo³², V. Trubnikov³, W.H. Trzaska¹¹⁴, T.P. Trzcinski¹³², R. Turrisi⁵³, T.S. Tveter¹⁹, K. Ullaland²⁰, B. Ulukutlu⁹⁶, A. Uras¹²⁵, M. Urioni^{54,130}, G.L. Usai²², M. Vala³⁷, N. Valle²¹, S. Vallero⁵⁵, L.V.R. van Doremalen⁵⁸, M. van Leeuwen⁸⁴, C.A. van Veen⁹⁵, R.J.G. van Weelden⁸⁴, P. Vande Vyvre³², D. Varga¹³⁵, Z. Varga¹³⁵, M. Varga-Kofarago¹³⁵, M. Vasileiou⁷⁸, A. Vasiliev¹³⁹, O. Vázquez Doce⁹⁶, V. Vechernin¹³⁹, E. Vercellin²⁴, S. Vergara Limón⁴⁴, L. Vermunt⁵⁸, R. Vértesi¹³⁵, M. Verweij⁵⁸, L. Vickovic³³, Z. Vilakazi¹²⁰, O. Villalobos Baillie¹⁰⁰, G. Vino⁴⁹, A. Vinogradov¹³⁹, T. Virgili²⁸, V. Vislavicius⁸³, A. Vodopyanov¹⁴⁰, B. Volkel³², M.A. Völkl⁹⁵, K. Voloshin¹³⁹, S.A. Voloshin¹³³, G. Volpe³¹, B. von Haller³², I. Vorobyev⁹⁶, N. Vozniuk¹³⁹, J. Vrláková³⁷, B. Wagner²⁰, C. Wang³⁹, D. Wang³⁹, M. Weber¹⁰², A. Wegrzynek³², F.T. Weiglhofer³⁸, S.C. Wenzel³², J.P. Wessels¹³⁴, S.L. Weyhmler¹³⁶, J. Wiechula⁶³, J. Wikne¹⁹, G. Wilk⁷⁹, J. Wilkinson⁹⁸, G.A. Willems¹³⁴, B. Windelband⁹⁵, M. Winn¹²⁷, J.R. Wright¹⁰⁷, W. Wu³⁹, Y. Wu¹¹⁷, R. Xu⁶, A.K. Yadav¹³¹, S. Yalcin⁷¹, Y. Yamaguchi⁹³, K. Yamakawa⁹³, S. Yang²⁰, S. Yano⁹³, Z. Yin⁶, I.-K. Yoo¹⁶, J.H. Yoon⁵⁷, S. Yuan²⁰, A. Yuncu⁹⁵, V. Zaccolo²³, C. Zampolli³², H.J.C. Zanoli⁵⁸, F. Zanone⁹⁵, N. Zardoshti^{32,100}, A. Zarochentsev¹³⁹, P. Závada⁶¹, N. Zaviyalov¹³⁹, M. Zhalov¹³⁹, B. Zhang⁶, S. Zhang³⁹, X. Zhang⁶, Y. Zhang¹¹⁷, M. Zhao¹⁰, V. Zhrebchevskii¹³⁹, Y. Zhi¹⁰, N. Zhigareva¹³⁹, D. Zhou⁶, Y. Zhou⁸³, J. Zhu^{98,6}, Y. Zhu⁶, G. Zinovjev^{1,3}, N. Zurlo^{130,54}

Affiliation Notes

- ^I Deceased
^{II} Also at: Max-Planck-Institut für Physik, Munich, Germany
^{III} Also at: Italian National Agency for New Technologies, Energy and Sustainable Economic Development (ENEA), Bologna, Italy
^{IV} Also at: Dipartimento DET del Politecnico di Torino, Turin, Italy
^V Also at: Department of Applied Physics, Aligarh Muslim University, Aligarh, India
^{VI} Also at: Institute of Theoretical Physics, University of Wrocław, Poland
^{VII} Also at: An institution covered by a cooperation agreement with CERN

Collaboration Institutes

- ¹ A.I. Alikhanyan National Science Laboratory (Yerevan Physics Institute) Foundation, Yerevan, Armenia
² AGH University of Science and Technology, Cracow, Poland
³ Bogolyubov Institute for Theoretical Physics, National Academy of Sciences of Ukraine, Kiev, Ukraine
⁴ Bose Institute, Department of Physics and Centre for Astroparticle Physics and Space Science (CAPSS), Kolkata, India
⁵ California Polytechnic State University, San Luis Obispo, California, United States
⁶ Central China Normal University, Wuhan, China
⁷ Centro de Aplicaciones Tecnológicas y Desarrollo Nuclear (CEADEN), Havana, Cuba
⁸ Centro de Investigación y de Estudios Avanzados (CINVESTAV), Mexico City and Mérida, Mexico
⁹ Chicago State University, Chicago, Illinois, United States
¹⁰ China Institute of Atomic Energy, Beijing, China
¹¹ Chungbuk National University, Cheongju, Republic of Korea
¹² Comenius University Bratislava, Faculty of Mathematics, Physics and Informatics, Bratislava, Slovak Republic
¹³ COMSATS University Islamabad, Islamabad, Pakistan
¹⁴ Creighton University, Omaha, Nebraska, United States
¹⁵ Department of Physics, Aligarh Muslim University, Aligarh, India
¹⁶ Department of Physics, Pusan National University, Pusan, Republic of Korea
¹⁷ Department of Physics, Sejong University, Seoul, Republic of Korea
¹⁸ Department of Physics, University of California, Berkeley, California, United States
¹⁹ Department of Physics, University of Oslo, Oslo, Norway
²⁰ Department of Physics and Technology, University of Bergen, Bergen, Norway
²¹ Dipartimento di Fisica, Università di Pavia, Pavia, Italy
²² Dipartimento di Fisica dell'Università and Sezione INFN, Cagliari, Italy
²³ Dipartimento di Fisica dell'Università and Sezione INFN, Trieste, Italy
²⁴ Dipartimento di Fisica dell'Università and Sezione INFN, Turin, Italy
²⁵ Dipartimento di Fisica e Astronomia dell'Università and Sezione INFN, Bologna, Italy
²⁶ Dipartimento di Fisica e Astronomia dell'Università and Sezione INFN, Catania, Italy
²⁷ Dipartimento di Fisica e Astronomia dell'Università and Sezione INFN, Padova, Italy
²⁸ Dipartimento di Fisica 'E.R. Caianiello' dell'Università and Gruppo Collegato INFN, Salerno, Italy
²⁹ Dipartimento DISAT del Politecnico and Sezione INFN, Turin, Italy
³⁰ Dipartimento di Scienze MIFT, Università di Messina, Messina, Italy
³¹ Dipartimento Interateneo di Fisica 'M. Merlin' and Sezione INFN, Bari, Italy
³² European Organization for Nuclear Research (CERN), Geneva, Switzerland
³³ Faculty of Electrical Engineering, Mechanical Engineering and Naval Architecture, University of Split, Split, Croatia
³⁴ Faculty of Engineering and Science, Western Norway University of Applied Sciences, Bergen, Norway
³⁵ Faculty of Nuclear Sciences and Physical Engineering, Czech Technical University in Prague, Prague, Czech Republic
³⁶ Faculty of Physics, Sofia University, Sofia, Bulgaria
³⁷ Faculty of Science, P.J. Šafárik University, Košice, Slovak Republic
³⁸ Frankfurt Institute for Advanced Studies, Johann Wolfgang Goethe-Universität Frankfurt, Frankfurt, Germany
³⁹ Fudan University, Shanghai, China
⁴⁰ Gangneung-Wonju National University, Gangneung, Republic of Korea
⁴¹ Gauhati University, Department of Physics, Guwahati, India

- ⁴² Helmholtz-Institut für Strahlen- und Kernphysik, Rheinische Friedrich-Wilhelms-Universität Bonn, Bonn, Germany
- ⁴³ Helsinki Institute of Physics (HIP), Helsinki, Finland
- ⁴⁴ High Energy Physics Group, Universidad Autónoma de Puebla, Puebla, Mexico
- ⁴⁵ Horia Hulubei National Institute of Physics and Nuclear Engineering, Bucharest, Romania
- ⁴⁶ Indian Institute of Technology Bombay (IIT), Mumbai, India
- ⁴⁷ Indian Institute of Technology Indore, Indore, India
- ⁴⁸ INFN, Laboratori Nazionali di Frascati, Frascati, Italy
- ⁴⁹ INFN, Sezione di Bari, Bari, Italy
- ⁵⁰ INFN, Sezione di Bologna, Bologna, Italy
- ⁵¹ INFN, Sezione di Cagliari, Cagliari, Italy
- ⁵² INFN, Sezione di Catania, Catania, Italy
- ⁵³ INFN, Sezione di Padova, Padova, Italy
- ⁵⁴ INFN, Sezione di Pavia, Pavia, Italy
- ⁵⁵ INFN, Sezione di Torino, Turin, Italy
- ⁵⁶ INFN, Sezione di Trieste, Trieste, Italy
- ⁵⁷ Inha University, Incheon, Republic of Korea
- ⁵⁸ Institute for Gravitational and Subatomic Physics (GRASP), Utrecht University/Nikhef, Utrecht, Netherlands
- ⁵⁹ Institute of Experimental Physics, Slovak Academy of Sciences, Košice, Slovak Republic
- ⁶⁰ Institute of Physics, Homi Bhabha National Institute, Bhubaneswar, India
- ⁶¹ Institute of Physics of the Czech Academy of Sciences, Prague, Czech Republic
- ⁶² Institute of Space Science (ISS), Bucharest, Romania
- ⁶³ Institut für Kernphysik, Johann Wolfgang Goethe-Universität Frankfurt, Frankfurt, Germany
- ⁶⁴ Instituto de Ciencias Nucleares, Universidad Nacional Autónoma de México, Mexico City, Mexico
- ⁶⁵ Instituto de Física, Universidade Federal do Rio Grande do Sul (UFRGS), Porto Alegre, Brazil
- ⁶⁶ Instituto de Física, Universidad Nacional Autónoma de México, Mexico City, Mexico
- ⁶⁷ iThemba LABS, National Research Foundation, Somerset West, South Africa
- ⁶⁸ Jeonbuk National University, Jeonju, Republic of Korea
- ⁶⁹ Johann-Wolfgang-Goethe Universität Frankfurt Institut für Informatik, Fachbereich Informatik und Mathematik, Frankfurt, Germany
- ⁷⁰ Korea Institute of Science and Technology Information, Daejeon, Republic of Korea
- ⁷¹ KTO Karatay University, Konya, Turkey
- ⁷² Laboratoire de Physique des 2 Infinis, Irène Joliot-Curie, Orsay, France
- ⁷³ Laboratoire de Physique Subatomique et de Cosmologie, Université Grenoble-Alpes, CNRS-IN2P3, Grenoble, France
- ⁷⁴ Lawrence Berkeley National Laboratory, Berkeley, California, United States
- ⁷⁵ Lund University Department of Physics, Division of Particle Physics, Lund, Sweden
- ⁷⁶ Nagasaki Institute of Applied Science, Nagasaki, Japan
- ⁷⁷ Nara Women's University (NWU), Nara, Japan
- ⁷⁸ National and Kapodistrian University of Athens, School of Science, Department of Physics, Athens, Greece
- ⁷⁹ National Centre for Nuclear Research, Warsaw, Poland
- ⁸⁰ National Institute of Science Education and Research, Homi Bhabha National Institute, Jatni, India
- ⁸¹ National Nuclear Research Center, Baku, Azerbaijan
- ⁸² National Research and Innovation Agency - BRIN, Jakarta, Indonesia
- ⁸³ Niels Bohr Institute, University of Copenhagen, Copenhagen, Denmark
- ⁸⁴ Nikhef, National institute for subatomic physics, Amsterdam, Netherlands
- ⁸⁵ Nuclear Physics Group, STFC Daresbury Laboratory, Daresbury, United Kingdom
- ⁸⁶ Nuclear Physics Institute of the Czech Academy of Sciences, Husinec-Řež, Czech Republic
- ⁸⁷ Oak Ridge National Laboratory, Oak Ridge, Tennessee, United States
- ⁸⁸ Ohio State University, Columbus, Ohio, United States
- ⁸⁹ Physics department, Faculty of science, University of Zagreb, Zagreb, Croatia
- ⁹⁰ Physics Department, Panjab University, Chandigarh, India
- ⁹¹ Physics Department, University of Jammu, Jammu, India
- ⁹² Physics Department, University of Rajasthan, Jaipur, India
- ⁹³ Physics Program and International Institute for Sustainability with Knotted Chiral Meta Matter (SKCM2), Hiroshima University, Hiroshima, Japan

- ⁹⁴ Physikalisches Institut, Eberhard-Karls-Universität Tübingen, Tübingen, Germany
⁹⁵ Physikalisches Institut, Ruprecht-Karls-Universität Heidelberg, Heidelberg, Germany
⁹⁶ Physik Department, Technische Universität München, Munich, Germany
⁹⁷ Politecnico di Bari and Sezione INFN, Bari, Italy
⁹⁸ Research Division and ExtreMe Matter Institute EMMI, GSI Helmholtzzentrum für Schwerionenforschung GmbH, Darmstadt, Germany
⁹⁹ Saha Institute of Nuclear Physics, Homi Bhabha National Institute, Kolkata, India
¹⁰⁰ School of Physics and Astronomy, University of Birmingham, Birmingham, United Kingdom
¹⁰¹ Sección Física, Departamento de Ciencias, Pontificia Universidad Católica del Perú, Lima, Peru
¹⁰² Stefan Meyer Institut für Subatomare Physik (SMI), Vienna, Austria
¹⁰³ SUBATECH, IMT Atlantique, Nantes Université, CNRS-IN2P3, Nantes, France
¹⁰⁴ Suranaree University of Technology, Nakhon Ratchasima, Thailand
¹⁰⁵ Technical University of Košice, Košice, Slovak Republic
¹⁰⁶ The Henryk Niewodniczanski Institute of Nuclear Physics, Polish Academy of Sciences, Cracow, Poland
¹⁰⁷ The University of Texas at Austin, Austin, Texas, United States
¹⁰⁸ Universidad Autónoma de Sinaloa, Culiacán, Mexico
¹⁰⁹ Universidade de São Paulo (USP), São Paulo, Brazil
¹¹⁰ Universidade Estadual de Campinas (UNICAMP), Campinas, Brazil
¹¹¹ Universidade Federal do ABC, Santo Andre, Brazil
¹¹² University of Cape Town, Cape Town, South Africa
¹¹³ University of Houston, Houston, Texas, United States
¹¹⁴ University of Jyväskylä, Jyväskylä, Finland
¹¹⁵ University of Kansas, Lawrence, Kansas, United States
¹¹⁶ University of Liverpool, Liverpool, United Kingdom
¹¹⁷ University of Science and Technology of China, Hefei, China
¹¹⁸ University of South-Eastern Norway, Kongsberg, Norway
¹¹⁹ University of Tennessee, Knoxville, Tennessee, United States
¹²⁰ University of the Witwatersrand, Johannesburg, South Africa
¹²¹ University of Tokyo, Tokyo, Japan
¹²² University of Tsukuba, Tsukuba, Japan
¹²³ University Politehnica of Bucharest, Bucharest, Romania
¹²⁴ Université Clermont Auvergne, CNRS/IN2P3, LPC, Clermont-Ferrand, France
¹²⁵ Université de Lyon, CNRS/IN2P3, Institut de Physique des 2 Infinis de Lyon, Lyon, France
¹²⁶ Université de Strasbourg, CNRS, IPHC UMR 7178, F-67000 Strasbourg, France, Strasbourg, France
¹²⁷ Université Paris-Saclay Centre d'Etudes de Saclay (CEA), IRFU, Département de Physique Nucléaire (DPhN), Saclay, France
¹²⁸ Università degli Studi di Foggia, Foggia, Italy
¹²⁹ Università del Piemonte Orientale, Vercelli, Italy
¹³⁰ Università di Brescia, Brescia, Italy
¹³¹ Variable Energy Cyclotron Centre, Homi Bhabha National Institute, Kolkata, India
¹³² Warsaw University of Technology, Warsaw, Poland
¹³³ Wayne State University, Detroit, Michigan, United States
¹³⁴ Westfälische Wilhelms-Universität Münster, Institut für Kernphysik, Münster, Germany
¹³⁵ Wigner Research Centre for Physics, Budapest, Hungary
¹³⁶ Yale University, New Haven, Connecticut, United States
¹³⁷ Yonsei University, Seoul, Republic of Korea
¹³⁸ Zentrum für Technologie und Transfer (ZTT), Worms, Germany
¹³⁹ Affiliated with an institute covered by a cooperation agreement with CERN
¹⁴⁰ Affiliated with an international laboratory covered by a cooperation agreement with CERN.